nr. 2/2006

Validating results from the model ROMS (Regional Ocean Modelling System), with respect to volume transports and heat fluxes in the Nordic Seas

Vidar S. Lien, Paul Budgell, Bjørn Ådlandsvik og Einar Svendsen

ISSN 0071 - 5638

PROSJEKTRAPPORT

HAVFORSKNINGSINSTITUTTET
INSTITUTE OF MARINE RESEARCH

Nordnesgaten 50, Postboks 1870 Nordnes, 5817 BERGEN
Tlf. 55 23 85 00, Fax 55 23 85 31, www.imr.no

Tromsø	Flødevigen	Austevoll	Matre
9294 TROMSØ	4817 HIS	5392 STOREBØ	5984 MATREDAL
Tlf. 55 23 85 00	Tlf. 37 05 90 00	Tlf. 55 23 85 00	Tlf. 55 23 85 00
Fax 77 60 97 01	Fax 37 05 90 01	Fax 56 18 22 22	Fax 56 36 75 85

Distribusjon:

HI-prosjektnr.:
VALDEMAR/11297

Oppdragsgiver(e):

Oppdragsgivers referanse:

Dato:
24.04.06

Program:

Forskningsgruppe:
Oseanografi og Klima

Antall sider totalt:
63

Rapport: FISKEN OG HAVET	**Nr. - År** 2 - 2006

Tittel (norsk/engelsk):
Validating results from the model ROMS (Regional Ocean Modelling System), with respect to volume transports and heat fluxes in the Nordic Seas

Forfatter(e):
Vidar S. Lien, Paul Budgell, Bjørn Ådlandsvik og Einar Svendsen

Sammendrag (norsk):

En 25 års modellsimulering med modellen ROMS (Regional Ocean Modelling System) er validert ved en kvantitativ sammenligning mellom modellresultater og observasjoner av temperatur og volumtransporter i De nordiske hav. I flere viktige snitt som er undersøkt, som Grønland-Skottland Ryggen, Svinøy-snittet og Framstredet, ligger modellresultatene innenfor usikkerhetene til observasjonene. Modellresultatene viser imidlertid en større variasjon enn observasjonene, både på årlige og mellomårlige tidsskalaer. Korrelasjonen mellom innstrømningen av Atlantisk vann inn i De nordiske hav og NAO-indeksen er relativt lav, noe som tyder på andre drivkrefter enn lokale vindfelt. Temperaturfeltene stemmer bra med observasjoner, og varmefluksene gjennom snittene som er undersøkte er sammenlignbare med estimater basert på observasjoner.

Summary (English):

A 25 year hindcast carried out with the model ROMS (Regional Ocean Modelling System) is validated by a quantitatively comparison between the model results and observations on temperatures and volume transports in the Nordic Seas. In several key sections investigated, including the Greenland-Scotland Ridge, the Svinøy section and the Fram Strait, the average modeled volume transports are within the uncertainties of observations. However, the model results show a larger variability than observations, both seasonally and interannually. The correlation between the NAO-index and the Atlantic inflow to the Nordic Seas is rather low, suggesting other possible driving forces than local winds. The temperature fields are well reproduced, and the heat fluxes through the sections investigated are comparable with estimates based on observations.

Emneord (norsk):	**Subject heading (English):**
1. Numerisk modellering	1. Numerical modelling
2. Validering	2. Validating
3. Nordiske hav	3. Nordic Seas

....
prosjektleder

....
forskningsgruppeleder

Validating results from the model ROMS (Regional Ocean Modelling System), with respect to volume transports and heat fluxes in the Nordic Seas

by

Vidar S. Lien, Paul Budgell, Bjørn Ådlandsvik and Einar Svendsen

Institute of Marine Research, Bergen, Norway

Abstract

A 25 year hindcast carried out with the model ROMS (**R**egional **O**cean **M**odelling **S**ystem) is validated by a quantitatively comparison between the model results and observations on temperatures and volume transports in the Nordic Seas. ROMS is a three-dimensional ocean general circulation model that uses a topography-following coordinate system in the vertical and orthogonal curvilinear coordinates in the horizontal.

In several key sections investigated, including the Greenland-Scotland Ridge, the Svinøy section and the Fram Strait, the average modeled volume transports are within the uncertainties of observations. However, the model results show a larger variability than observations, both seasonally and interannually. The correlation between the NAO-index and the Atlantic inflow into the Nordic Seas is rather low, suggesting other possible driving forces than local winds. The temperature fields are well reproduced, and the heat fluxes through the sections investigated are comparable with estimates based on observations. An increased northward heat flux through the Fram Strait in the 1990s, which caused a warming of the Arctic, is reproduced by the model. Also single events such as volume transport anomalies on monthly time scales are captured in the model results.

Contents

Chapter 1

Introduction

The flow of warm and saline Atlantic Water from the Atlantic Ocean into the Nordic Seas and the Arctic Ocean, collectively termed the Arctic Mediterranean, is of great importance both for the regional climate and for the global thermohaline circulation. The study of the inflow of Atlantic Water into the Nordic Seas has therefore been given much attention during recent decades. A general picture of the flow pattern in the Nordic Seas is established (figure 4.1), and estimates of the total inflow of Atlantic Water into the Arctic Mediterranean have been calculated, e.g. (Østerhus et al. 2005), (Girton et al. 2001) and (Dickson et al. 1999). Earlier estimates of the volume fluxes of Atlantic inflow were based on budgets, e.g. Worthington (1970). However, more recently, several arrays of moored current meters and cruises conducting CTD-casts and ADCP-sections have opened the possibilities for more direct calculations of the Atlantic inflow, e.g. Østerhus et al. (2005).

Numerical modelling is a powerful tool when looking at the state of the ocean. The great advantage of a numerical model is that it opens up the possibility to investigate the ocean in all four dimensions; the three spatial dimensions in addition to time. In this way, a numerical model is able to give far more information than observations. However, in order to use these enormous amounts of data, it is very important to know wether the model results give a realistic representation of the ocean.

The aim of this work is to quantify the total volume transport in the Nordic Seas and the inflow of Atlatic Water into the Nordic Seas, by the use of an ocean general circulation model. The model used is ROMS, **R**egional **O**cean **M**odelling **S**ystem. Model results from a 25 year hindcast are available and the model performance is validated with respect to water mass characteristics and the general circulation in the Nordic Seas. To do this, several key sections have been chosen where observations are available, and the model results are compared with existing litteratue on observations. Examples of such key areas are the Greenland-Scotland Ridge, e.g. Østerhus et al. (2005), the Svinøy section, e.g. Orvik et al. (2001) and the Fram Strait, e.g. Schauer et al. (2004). Only a brief and general description of the general circulation pattern in the Nordic Seas will be given, and the model results, with respect to these general features, are highlighted. In this text, all water masses entering the Nordic Seas are termed “inflow”, and all water masses leaving the Nordic Seas are termed “outflow”. Within the Nordic Seas, northward and eastward flow are termed “inflow” and southward and westward flow are termed "outflow". When using the term "Nordic Seas", the Barents Sea is not included here, and thus the Nordic Seas means the so-called GIN Seas; the Greenland, Iceland and the Norwegian Seas.

In the following sections, the model ROMS and the model setup used in this run is briefly described. Then a presentation of some of the model results and a comparison between model results and literature on observed data is given, starting with the inflow of Atlantic Water over the Greenland-Scotland Ridge. The total flow in the Nordic Seas is examined, with special interest put in the East Greenland Current, and a budget for the total volume fluxes through the Nordic Seas is given. Then heat fluxes through the different sections are computed, and a heat budget for the Nordic Seas is presented. The heat fluxes through the sections closing the Nordic Seas basin are compared with observed heat fluxes and fluxes based on budgets. Due to a sign error in the precipitation-evaporation balance, the surface layers becomes fresher as time evolves, and salinity is therefore not included in this work. However, in the last section, some results regarding the salinity is presented. Due to the amount of presented data and results, the results are presented and discussed separately for each section. Finally, a summary and some conclusions are made.

Chapter 2

Model Description

ROMS is a three dimensional baroclinic ocean general circulation model (OGCM) that uses a terrain-following coordinate system in the vertical. This allows an enhanced resolution both near the surface and near the bottom, and gives a good resolution of the processes near the surface and on the shelves. In the horizontal, ROMS uses orthogonal curvilinear coordinates. The development of ROMS is described in several papers; Song & Haidvogel (1994), Haidvogel & Beckmann (1999), Haidvogel et al. (2000), Shchepetkin & McWilliams (2003) and Shchepetkin & McWilliams (2005).

2.1 Model run

The model domain used in this run is shown in figure 2.1. The model uses a stretched spherical coordinate grid in the horizontal (Bentsen et al. 1999), with the "North Pole" situated in central Asia and the "South Pole" situated in the Pacific Ocean. This gives the model an increased resolution in desired areas (see figure 2.1). In the vertical, there are 30 generalized sigma (s) coordinate layers, stretched to increase the vertical resolution near the surface and the bottom. A time step of 900 s is used. There are no tides, and the vertical mixing scheme used is the LMD parametrization (Large et al. 1994). The lateral boundaries are closed. However, a constant volume flux of 1 Sv (1 Sv = 10^6 m^3/s) is input through the Bering Strait and 1 Sv is removed from the southern boundary. NCEP wind stress is used as atmospheric forcing, obtained from the NCEP/NCAR reanalysis data (Kalnay et al. 1996). Daily mean wind stress and latent, sensible, downward shortwave radiative and net longwave radiative heat fluxes were applied as surface forcing after correcting for differences in model and NCEP surface conditions, such as in surface temperature and ice concentration. The flux corrections applied were developed by Bentsen & Drange (2000) and provide a feedback between the model surface temperature and applied heat fluxes, thus minimizing problems with drift in model surface temperatures. Precipitation is taken from the daily mean NCEP values, and snowfall is taken to be precipitation, corrected for snow density, when air temperature is less than 0 ^oC. Evaporation is computed from the latent heat flux. River runoff is computed using the NCEP/NCAR reanalysis daily accumulated surface runoff values over land that are routed to ocean discharge points using the Total

Runoff Integrated Pathways (TRIP) approach of Oki & Sud (1998).

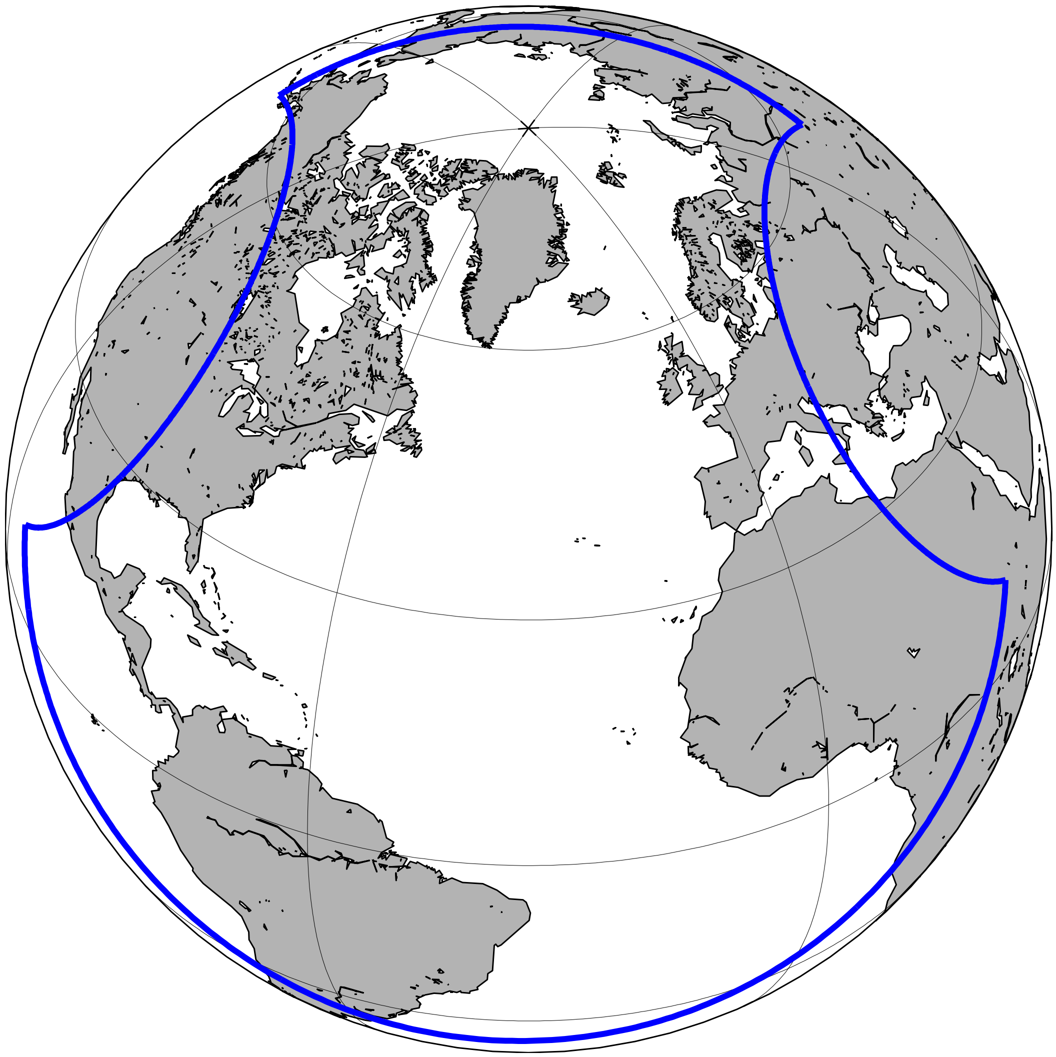

Figure 2.1: ***Model domain.***

The model is run for 25 years, from 1981 to 2005. A coarser model, with a resolution of about 50 km, has been used as starting field for the current model run. Thus, the model should require only a short spin-up time. The horizontal resolution in the area studied is about 20 km, and a loss of small scale eddy-activity is therefore expected. The data are averaged to monthly means before they are analyzed, and this should anyway smooth out most of the small scale eddy-activity.

Chapter 3

Methods

Figure 3.1 shows the Nordic Seas with bathymetry. The different sections discussed in this work are shown as red lines (see appendix for names and positions of the sections).

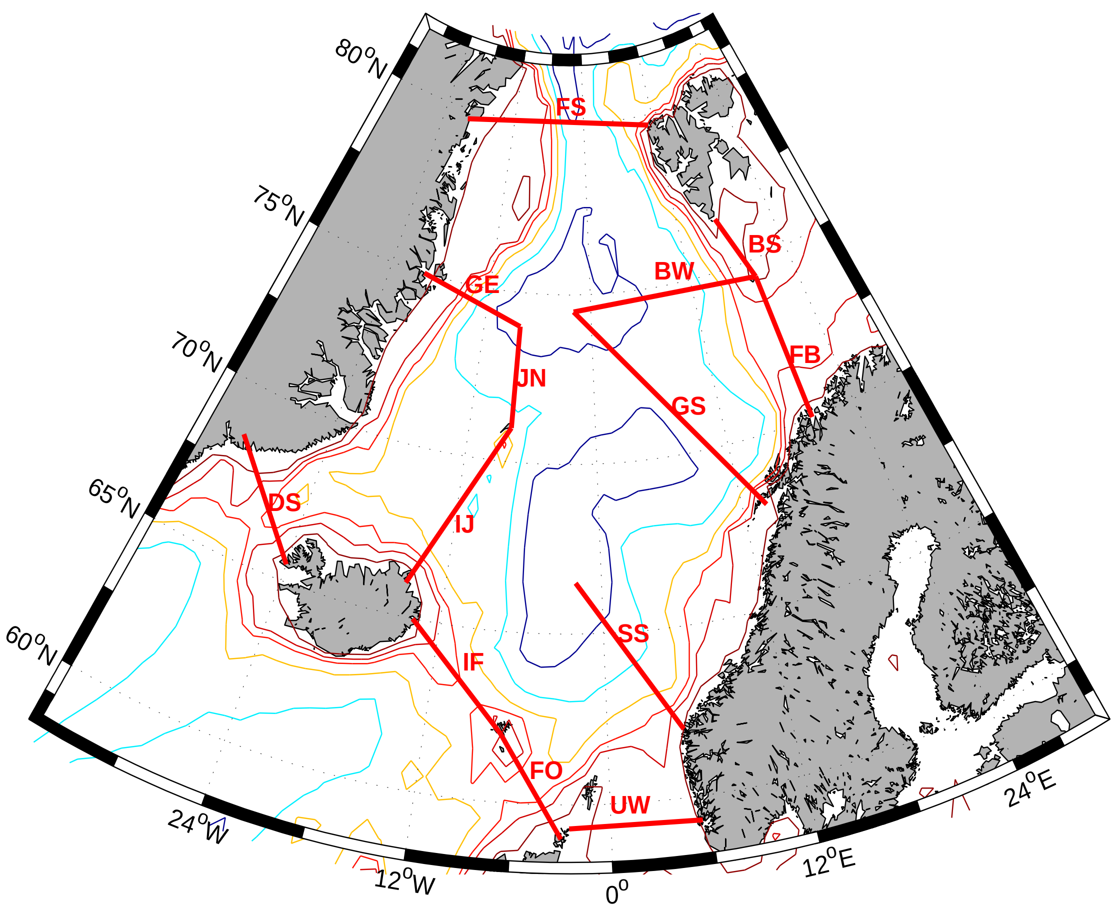

Figure 3.1: ***Map and bathymetry of the area investigated. The red lines show the different sections discussed, with the corresponding abbreviations.***

All sections analyzed in this work are placed solely for the purpose of this work. The sections at the borders of the Nordic Seas are placed in order to close the basin. Thus, the positions of the sections in this work may differ from the positions of observed sections. Volume transports in both directions have been calculated in all sections. In key sections, also flow speed, mean temperature and heat fluxes are calculated. Matlab has been used in all processing and calculations.

Chapter 4

General circulation

This section summarizes the general flow pattern in the Nordic Seas.

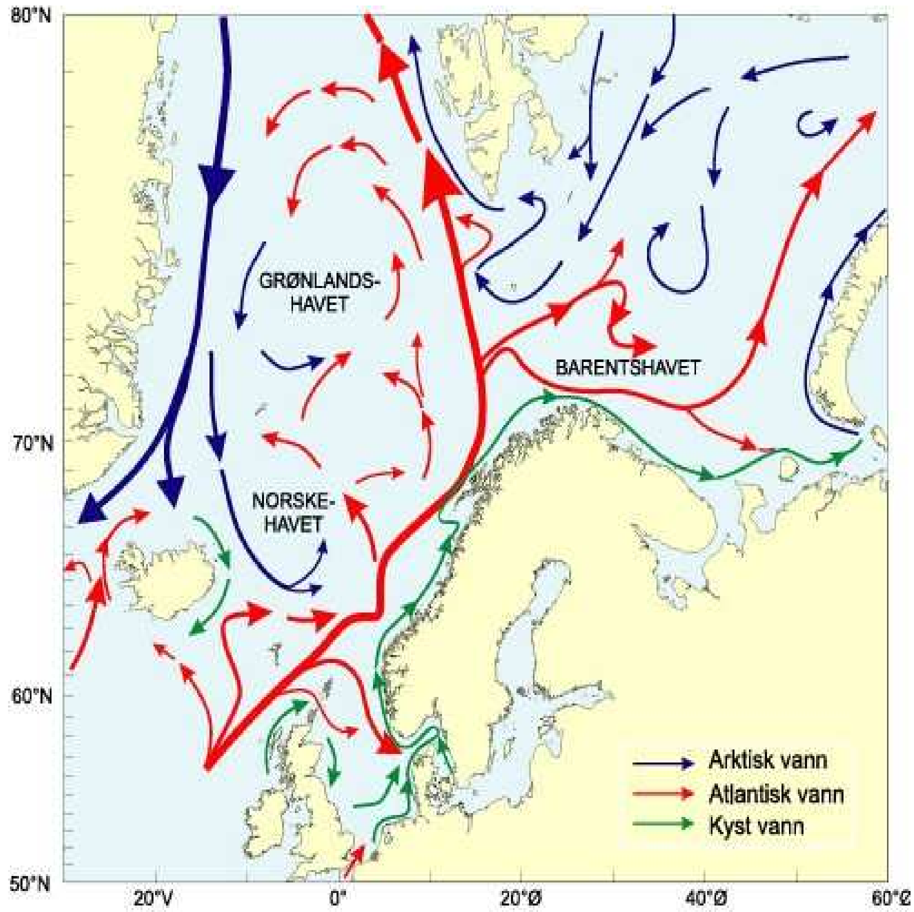

Figure 4.1: ***Map showing the general circulation pattern in the Nordic Seas. Red arrows are inflow of warm Atlantic Water, blue arrows are cold Arctic water and green arrows are coastal water.***

Figure 4.1 shows the general circulation pattern in the Nordic Seas, based on direct current measurements and hydrography. The figure shows the warm Atlantic inflow in the eastern part of the basin, with two main branches, one east and one west of the Faroe Islands. The Atlantic inflow follows the norwegian shelf, with one part flowing into the Barents Sea, while the other part continues northward along the western part of Spitsbergen and finally enters the Arctic through the Fram Strait. A compensating southward flow of cold Arctic Water is flowing out of the Arctic through the Fram Strait. This flow continues southward along the Greenland shelf, and finally enters the Atlantic through the Denmark Strait between Greenland and Iceland.

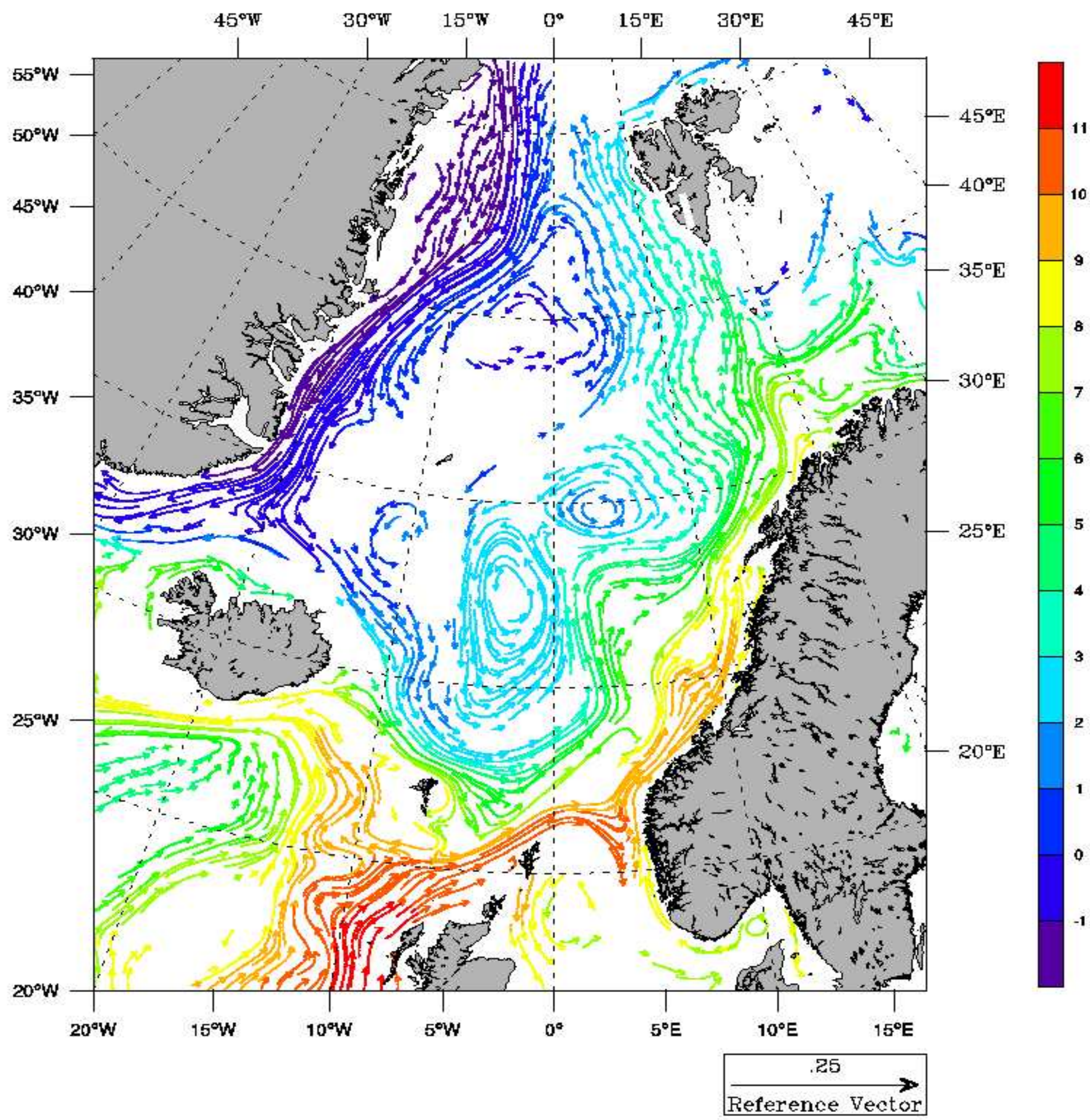

Figure 4.2: ***Mean modeled velocity field in the Nordic Seas. The length of the vectors denote current speed and colors denote temperature. Velocities below 2 cm/s are not shown. The field show the 1981-2004 average at 50 meter depth.***

In figure 4.2, the corresponding modeled circulation in the Nordic Seas is shown. The vectors show the circulation pattern, the length of the vectors denote velocity and the color denote temperature. The field show the 1981-2004 average at 50 meter depth. Main features as seen in figure 4.1, such as the Atlantic inflow over the Greenland-Scotland Ridge and through the Svinøy section, the exchanges through the Fram Strait and the outflow of cold surface water through the Denmark Strait are all clearly seen. Even the Norwegian Coastal Current is visible, despite the relatively coarse model resolution. Note also the two branch structure of the Atlantic inflow along the norwegian shelf.

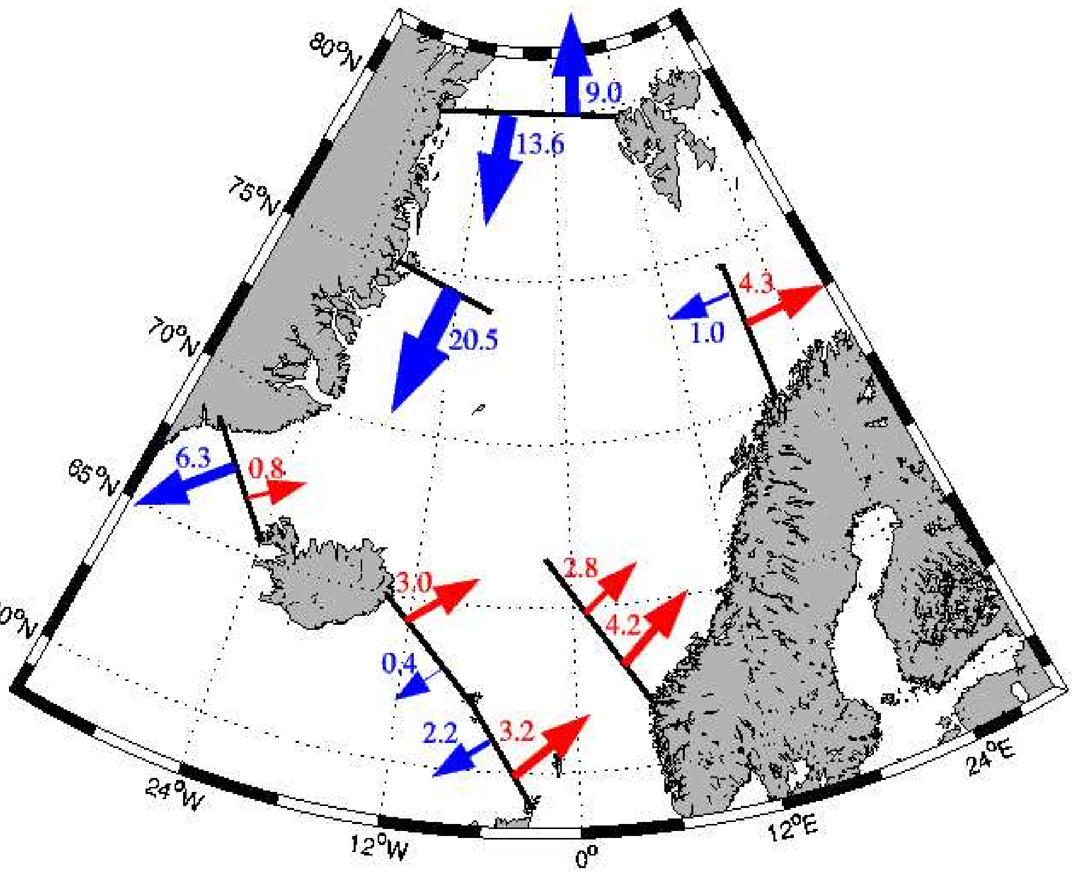

Figure 4.3: ***Volume transports through the Nordic seas. Red arrows denote Atlantic inflow. Blue arrows denote colder water masses.***

Figure 4.3 shows the volume transports through the Nordic seas calculated from the model results. The calculations are based on the average for the whole modeled period, 1981-2005.

Chapter 5

Atlantic inflow

The inflow of warm and saline Atlantic Water into the Nordic Seas is having a huge impact on the climate in northern Europe. Virtually all Atlantic Water in the Nordic Seas and Arctic Ocean enters over the Greenland-Scotland Ridge (see map, figure 4.1). Therefore, a lot of research has been conducted in order to quantify the Atlantic inflow over the Greenland-Scotland Ridge, and several arrays of moored current meters have been deployed between Shetland and the Faroes, north of the Faroes and north of Iceland, in order to monitor the Atlantic inflow through the three passages. By the use of both budgets e.g. Worthington (1970), observations e.g. Østerhus et al. (2005) and numerical models e.g. Nilsen et al. (2003), several estimates of the Atlantic inflow have been calculated. Usually, Atlantic Water is defined as water masses with salinities above 35.0 psu (Helland-Hansen & Nansen 1909). Due to the error in the salinity fields as mentioned earlier, salinity has not been used to define water masses in this work. Another characteristic of Atlantic Water is higher temperatures compared to other water masses in the Nordic Seas. Observations show that 5 ^{o}C corresponds to salinities of 35.0 psu in the Atlantic inflow (Orvik et al. 2001). Therefore, Atlantic Water is here defined as water masses with temperature equal to or above 5 ^{o}C.

5.1 Greenland-Scotland Ridge

The Greenland-Scotland Ridge is divided into three sections; The Faroe-Shetland Channel, which is the deepest of the three sections, The Iceland-Faroe Ridge and the Denmark Strait between Iceland and Greenland. All the sections are shown in figure 3.1. Recirculation of Atlantic Water due to eddy-activity and topographical steering along the Greenland-Scotland Ridge makes it difficult to estimate the real transport of Atlantic Water into the Nordic Seas without classifying the different water masses passing through the different sections. Atlantic Water flowing southward in the three sections across the Greenland-Scotland Ridge is removed from the total Atlantic inflow when calculating the net Atlantic inflow through the different sections. In this work, a section stretching from the Faroes to the Orkney is chosen to represent the Faroe-Shetland Channel. The section across the Denmark Strait is placed across the shallowest part of the Strait, in order to omit most of the possible recirculation. The inflow between Iceland and the Faroes is usually observed in a section north of the

Faroes. However, in this work, the section is placed in a straight line between Iceland and the Faroes, in order to close the Nordic Seas basin.

5.1.1 Results

Figure 5.1 shows the modeled net Atlantic inflow through the three sections at the Greenland-Scotland Ridge. With the 3-year moving averages ranging from 1.7 Sv in the mid-1980s to 4.4 Sv in 2001, and the monthly averages ranging from 2.2 Sv in June/July to 4.1 Sv in January, the inflow through the Faroe-Shetland Channel shows the largest variability, both seasonally and interannually.

Figure 5.1: ***3-Year moving averages of net Atlantic inflow (left) and monthly average net Atlantic inflow (right) through the three sections.***

Figure 5.2 shows the net Atlantic inflow through the Faroe-Shetland Channel. As can be seen in the figure, it seems to be both a seasonal signal and a large interannual variability. Note also the very large inflow in winter 1993, with the volume flux reaching 9.3 Sv in January. This is clearly a single, distinct event. However, all high inflow events ocurrs in winter. At one occasion (November 1985), there is a net outflow of Atlantic Water in the section. Overall, the model gives an average net Atlantic inflow of 3.2 Sv, with a standard deviation of 1.5 Sv. The large standard deviation, compared to the average, reflects the variability of the inflow. If the recirculation in the section is neglected and the total inflow is computed, the average inflow rises to 6.0 Sv. However, the standard deviation is reduced to 1.1 Sv. Thus, including the recirculation seems to contribute to a more steady inflow.

Figure 5.3 shows the net Atlantic inflow over the Iceland-Faroe Ridge, and shows a high variability both seasonally and interannually, although the differences are smaller than in the Faroe-Shetland Channel. Some striking features include a very sharp change from low inflow in 1988 to high inflow in 1989, and very low inflow in January 1993, when the highest peak ocurred in the Faroe-Shetland Channel. Overall, the model gives a net Atlantic inflow of 3.0 Sv with a standard deviation of 1.0 Sv. The total inflow amounts to 4.4 Sv, with a standard deviation of 0.9 Sv.

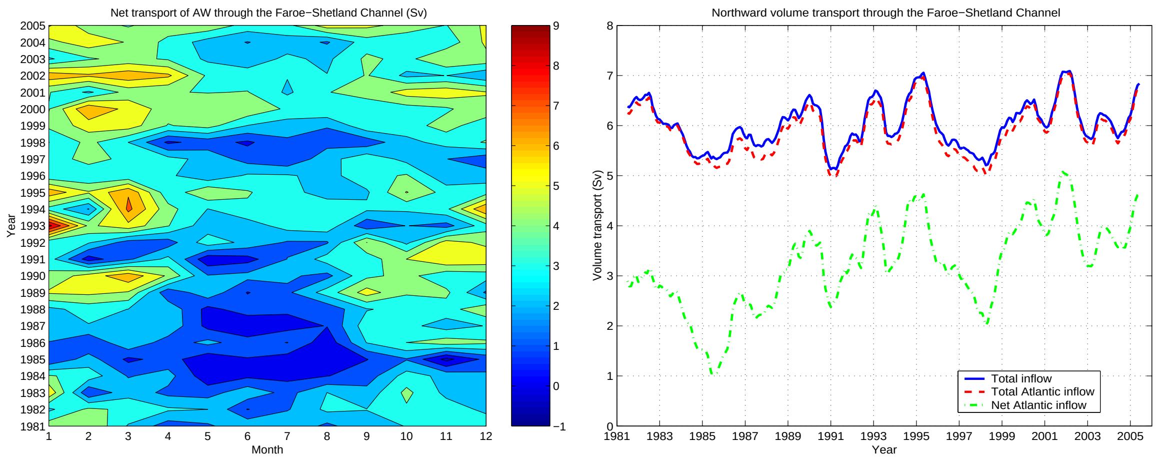

Figure 5.2: ***Faroe-Shetland Channel. Left: Net inflow of Atlantic Water. Right: Yearly moving averages of total inflow, Atlantic inflow and net Atlantic inflow.***

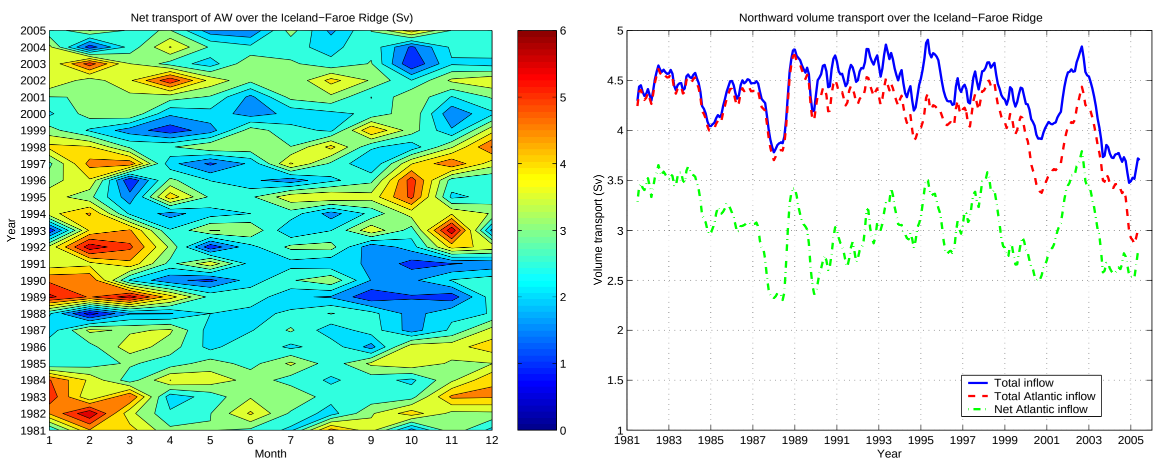

Figure 5.3: ***Iceland-Faroe Ridge. Left: Net inflow of Atlantic Water. Right: Yearly moving averages of total inflow, Atlantic inflow and net Atlantic inflow.***

Figure 5.4 shows the net Atlantic inflow through the Denmark Strait. An average of 0.8 Sv with a standard deviation of 0.3 Sv, is found. In November 1986 and October 1995, there is a net outflow of Atlantic Water through the section. The largest inflow is found in late spring/early summer, while winter values show a larger variability. Generally, the inflow is lower in winter, but the two largest peaks is found in February, with 1.6 Sv in 1985 and 1991. The total inflow is 1.6 Sv on average, with a standard deviation of 0.4 Sv.

Total inflow, Atlantic inflow and net Atlantic inflow are summarized in table 5.1. In both the Faroe-Shetland Channel and the Iceland-Faroe Ridge, the Atlantic inflow is very close to the total inflow. The net Atlantic inflow is, however, substantially lower, indicating that some recirculation is taking place and/or some eddy activity in the area. In the Denmark Strait, there seems to be very little recirculation of Atlantic Water. However, a substantial part of the inflow is obviously Atlantic Water with temperatures below 5 ^{o}C.

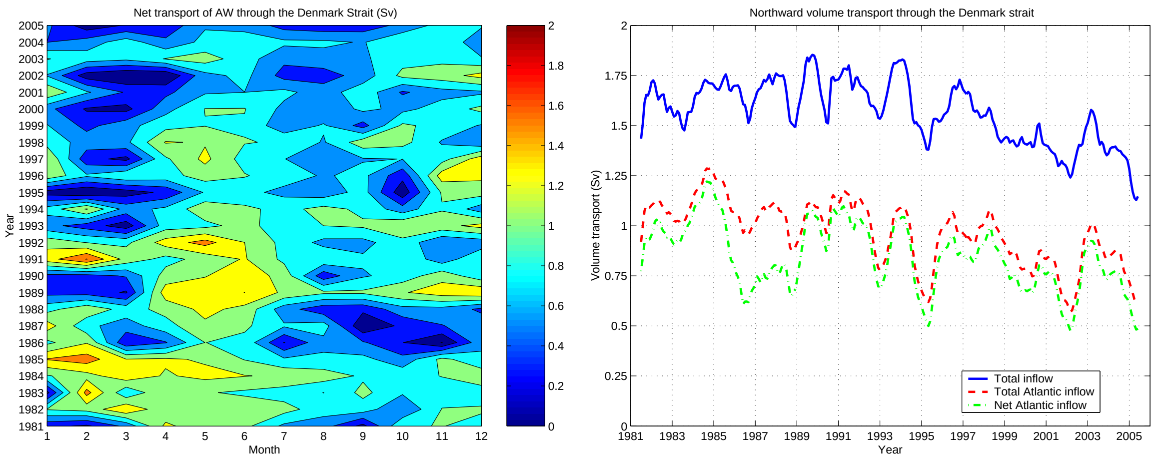

Figure 5.4: ***Denmark Strait. Left: Net inflow of Atlantic Water. Right: Yearly moving averages of total inflow, Atlantic inflow and net Atlantic inflow.***

Section	Total inflow	Atlantic inflow	Net Atlantic inflow
Faroe-Shetland Channel	6.0	5.9	3.2
Iceland-Faroe Ridge	4.4	4.1	3.0
Denmark Strait	1.6	1.0	0.8
Total	12.0	11.0	7.0

Table 5.1: ***Modeled inflow over the Greenland-Scotland Ridge.***

In order to quantify the consistency in the seasonal signal, correlation coefficients between the monthly means for each year and the modeled climatological monthly means for the net Atlantic inflow through the three sections, have been computed. The correlation coefficients are found to be 0.54 on average for the Faroe-Shetland Channel, with positive values in all years, 0.31 on average for the Iceland-Faroe Ridge; highly variable with values down to -0.6, and 0.41 on average for the Denmark Strait, with the only negative values in 1991 and 2004. These values are around 0.1 lower than the values computed from the total inflow through the three sections. Thus, the Faroe-Shetland Channel is the only section where the inflow show a fairly consistent seasonal variation with the higher inflow in winter. In the Denmark Strait, the seasonal signal is weaker, and also in opposite phase, with the higher values in summer, while it is impossible to conclude whether there is any seasonal signal on the Iceland-Faroe Ridge.

5.1.2 NAO

Wind is a major driving force of currents in the upper layers, and the North Atlantic Oscillation (NAO) may therefore greatly influence the flow over the Greenland-Scotland Ridge. Monthly means and yearly moving averages of the NAO-index are shown in figure 5.5 (left), while winter values (December through March) of the NAO-index are shown to the right.

The NAO data are from http://www.cgd.ucar.edu, and are based on the normalized difference in sea-level pressure between Lisbon, Portugal and Reykjavik, Iceland. The winter index is available for all years, while the monthly data are available only up to 2002. The correlations between the NAO-index and the modeled inflow through the three sections on the Greenland-Scotland Ridge are shown in table 5.2.

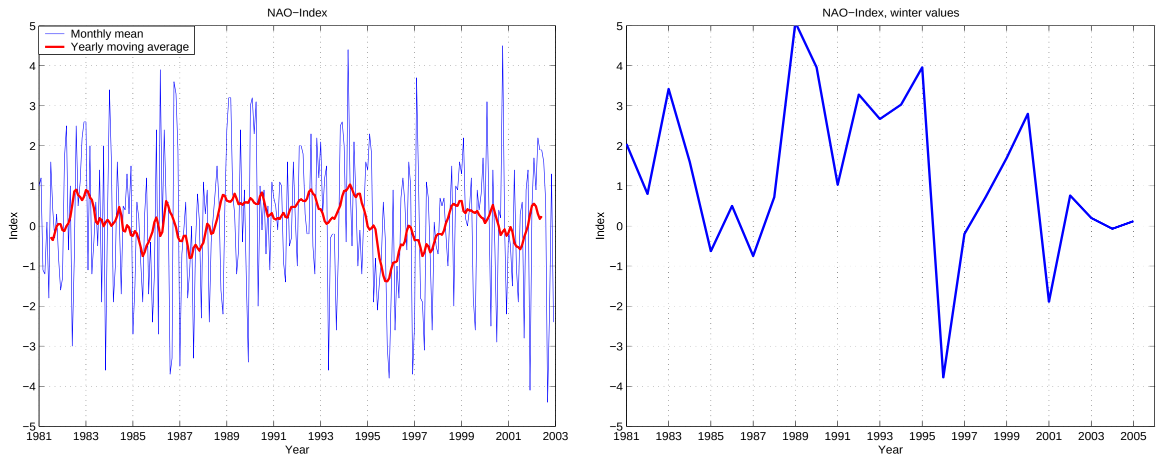

Figure 5.5: ***Left: Monthly averages and yearly moving average of NAO index for the period 1981 to 2002. Right: Winter values of the NAO-index, the months Dec, Jan, Feb and Mar are included.***

Section	Monthly means	Winter values
Faroe-Shetland Channel	0.36	0.40
Iceland-Faroe Ridge	0.28	0.49
Denmark Strait	-0.33	-0.40

Table 5.2: ***Correlation coefficients between net Atlantic inflow and NAO index.***

5.1.3 Discussion

The net Atlantic inflow shown in table 5.1, show that the two branches east of Iceland are the main contributors to the Atlantic inflow to the Nordic Seas. This is in agreement with observations, see e.g. Hansen & Østerhus (2000). Also the volume fluxes in all three branches are in fairly good agreement with observations. Table 5.3 compares the modeled data with different observations and also one other model experiment by the use of the model system MICOM (**M**iami **I**sopycnic **C**oordinate **O**cean **M**odel), conducted by Nilsen et al. (2003).

Table 5.3 shows that the modeled volume fluxes presented here are generally lower than observed values. However, these model results represent the whole modeled period, 1981-2005, while the observations only include time series from late 1990s until around 2001. Østerhus et al. (2005) operates with an uncertainty of 1 Sv on the total inflow over the

	Modeled		Estimated from observations			
Section	ROMS	N(2003)	HØ(2000)	T(2003)	H(2003)	Ø(2005)
FS	3.2	4.4		3.2		3.8
IF	3.0	2	3.3		3.5	3.8
DS	0.8	0.5	1.0			0.8
Total	7.0	6.9				8.5

Table 5.3: ***Modeled and observed values for net Atlantic inflow over the Greenland-Scotland Ridge. N(2003)=Nilsen et al, 2003. HØ(2000)=Hansen and Østerhus, 2000. T(2003)=Turrell et al, 2003. H(2003)=Hansen et al, 2003. Ø(2005)=Østerhus et al, 2005.***

Greenland-Scotland Ridge. When this uncertainty and the interannual variability is taken into consideration, the model results are quite close to the observed volume transports. Including only the years 1999-2001, which are the years of measurements Østerhus et al. (2005) base their findings on, the following volume transports are found in the model: 4.2 Sv in the Faroe-Shetland Channel, 2.7 Sv over the Iceland-Faroe Ridge and 0.7 Sv through the Denmark Strait; a total of 7.6 Sv, which is within the uncertainty of the 8.5 +/-1 Sv found by Østerhus et al. (2005). On the other hand, the model show a larger fraction of the inflow coming through the Faroe-Shetland Channel in these years than what is estimated from observations.

Two other factors that may play important roles, are how the inflow is defined and where the section is placed. The first regards which water masses are accounted for and how eddy-activity and recirculation is treated, and the latter regards which currents are accounted for and how much influence the eddy-activity and recirculation will have. In this work, all three sections are placed across the shallowest parts of each of the three passages. This in order to omit most of the topographically steered recirculation within the passage, and also to catch all inflow and outflow through each section and close the Nordic Seas basin. However, inspection of vertical sections through the three passages indicate some eddy-activity on the Iceland-Faroe Ridge and some recirculation in the Faroe-Shetland Channel. In the Denmark Strait, the inflow and outflow seems to consist of totally different water masses and are easily distinguishable. Thus, both the total inflow and outflow through the Denmark Strait would have been good approximations of the net inflow and outflow, respectively. A section north of the Faroes is often used to measure the inflow over the Iceland-Faroe Ridge. This will remove most of the influence of eddy-activity and recirculation on the Ridge, but it may also include some Atlantic Water from the Denmark Strait inflow, especially when water masses are defined solely by temperature. Therefore, higher inflow may be expected through the northward section than through the section along the Ridge.

As an example of the importance of defining the water masses, I will compare these model results with the model results by Nilsen et al. (2003). In this work, net Atlantic inflow is defined as net inflow of water with temperatures above 5 ^{o}C, where all outflow of these water masses are considered recirculation and is therefore subtracted from the total Atlantic inflow.

This gives a total inflow of 4.4 Sv and a net Atlantic inflow of 3.0 Sv over the Iceland-Faroe Ridge. In the model experiment done by Nilsen et al. (2003), the total inflow through this section was found to be 5.6 Sv, while a high outflow of 3.6 Sv gave a net inflow is 2 Sv. However, no temperature criterion was used, and these two net inflows may therefore not be directly compared.

As seen in figures 5.2 to 5.4, there seems to be some seasonal signal in the inflow through the three sections. Østerhus et al. (2005) found no significant seasonal variation in the flow pattern in the two branches east of Iceland, while the inflow through the Denmark Strait had a seasonal amplitude significantly different from zero. They also found that the inflow through the Faroe-Shetland Channel showed the largest variability. However, it was uncertain whether this variability was realistic, or if it was due to differences in the precision of the estimates. In the model results, the Shetland branch shows the largest variability both seasonally and interannually. To investigate the possible seasonal differences, summer and winter averages of the inflow have been computed. The three first and the three last months of the year have been used to calculate the winter averages, while the summer averages consist of the months April through September. To quantify the seasonal difference in Atlantic inflow, the differences and standard deviations of the differences between the winter and summer averages are calculated. The section that shows the largest seasonal variability, is the Faroe-Shetland Channel, with an average difference of 1.1 Sv between summer and winter. The standard deviation is 0.8 Sv, or about 70 % of the total difference. On the Iceland-Faroe Ridge, the seasonal signal is weaker. On average, the difference between winter and summer is 0.5 Sv, with the higher inflow in winter. The standard deviation is, however, 0.6 and thus larger than the average difference. The difference is also negative in some years. In the Denmark Strait, the difference between winter and summer inflow is -0.1, with a standard deviation of 0.2. Thus, the inflow through the Denmark Strait has the highest values in summer, but the standard deviation is also here higher than the average seasonal difference, and the difference also gives positive values in some years. It is thus impossible to conclude whether the inflow through the Denmark Strait and over the Iceland-Faroe Ridge show any seasonal variability, while the seasonal variability in the inflow through the Faroe-Shetland Channel has an average difference between summer and winter which is larger than the standard deviation. Thus, it is reasonable to say that the Shetland branch show a seasonal signal. However, the standard deviation of the winter and summer means are 1.1 Sv and 1.0 Sv, respectively. This may imply that the seasonal signal is masked by the interannual variability, and that the interannual variability is on the same order of magnitude as the seasonal variability. This is supported by looking at yearly averages and the standard deviation of the interannual variability. As the winter is the season with the highest inflow, each year is centered around the winter, so that each year span from July one year to June the next year. In this way, the whole winter season with corresponding low pressure activity is kept within the same year. Yearly average net Atlantic inflow ranges from 1.4 Sv in 1985/86 to 5.0 Sv in 2001/02. A standard deviation of 0.9 Sv is found between the years, which is close the average difference of 1.1 Sv between summer and winter values.

In the other two sections, the interannual variability is smaller than in the Faroe-Shetland Channel, with standard deviations of 0.4 Sv and 0.2 Sv for the Iceland-Faroe Ridge and the Denmark Strait, respectively. Thus, the difference between summer and winter values are on the same order of magnitude as the standard deviations between the years in both sections, but the variability is smaller relative to the inflow in the two latter sections. However, the difference between two following years are on the order of two standard deviations on several occasions in all three sections. This also gives relatively large fluctuations on the yearly net Atlantic inflow over the Greenland-Scotland Ridge (figure 5.6).

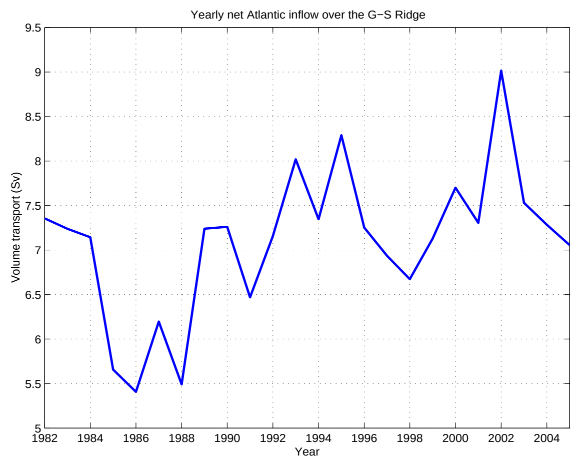

Figure 5.6: ***Yearly net Atlantic inflow over the Greenland-Scotland Ridge. The averages are from July to June.***

Although variations on a time scale shorter than a couple of months are impossible to detect using monthly averages, there are some traces of such fluctuations also in this data set. The most spectacular event is the extremely large inflow through the Faroe-Shetland Channel in January 1993, with the total inflow reaching 10.8 Sv. The corresponding net Atlantic inflow is 9.3 Sv, which is almost three times the average net Atlantic inflow, even in winter. My suggestion to why this anomalously high inflow ocurred, is that an extremely intense low pressure system with corresponding very strong winds crossed the area in January 1993. However, this is not seen in the NAO index. It is also an interesting observation that the net Atlantic inflow over the Iceland-Faroe Ridge was correspondingly low at the same time (see figures 5.2 and 5.3). During the years 1985/86, when the lowest inflow in the Faroe-Shetland Channel ocurred, one month, November 1985, show a slightly negative net inflow of Atlantic Water. In the Denmark Strait, there are two events of negative monthly net Atlantic inflow during the whole time series. On the Iceland-Faroe Ridge, no such event ocurrs.

From figure 5.1, it is clear that the Denmark Strait inflow is seasonally in counter-phase with the other two sections. In fact, while the two other inflows have larger values in winter than in summer, the Denmark Strait inflow show a dipole structure, with the largest peak in May, and a lower peak in November/December. Two minima are found, one in March and a second in August/September. Another interesting observation, is a seemingly shift in the seasonal variation in the inflow through the Denmark Strait. At the start of the time series, the largest values are found in February/March and decreasing through the year. After 1985, however, the largest inflow is generally found around May/June. Computing correlations between the seasonality each year and the climatological seasonality, gives an average correlation coefficient of 0.41. The correlation is positive for all years except 1991 and 2004, when there is a small negative correlation. In the years 1982 to 1985 the correlations are below 0.25. This indicates a fairly consistent seasonal signal, except for the mid-1980s, as mentioned. Jonsson & Valdimarsson (2004) conclude that although there is no seasonal signal in the current velocity, the Atlantic Water fraction varies seasonally and gives rise to a seasonal amplitude of 0.2 Sv, with a maximum in September. In the model, the maximum is seen in May/June, while September is close to the minimum inflow.

According to both observations (Østerhus et al. 2005) and model results (Nilsen et al. 2003), there is a negative correlation between the Atlantic inflow between Greenland and the Faroes and the Atlantic inflow between the Faroes and Shetland. This is partly explained by the influence of the NAO, which represents the mean wind stress in the North Atlantic. A positive NAO-index will tend to push water northeastward, mainly through the Faroe-Shetland Channel, but also over the Iceland-Faroe Ridge, depending on the position of the Icelandic low. On the other hand, a positive NAO will give northerly winds in the Denmark Strait, blocking the inflow through this section but allowing a larger outflow. A negative NAO-index will act in the opposite way; reducing the inflow east of Iceland and increasing the inflow west of Iceland. This pattern is poorly resolved in these model results. The correlation between the total inflow between Greenland and the Faroes and the inflow in the Faroe-Shetland Channel, is as low as -0.24. However, the value is negative, which gives an indication of the pattern. There is no correlation between the Iceland-Faroe Ridge inflow and the Faroe-Shetland Channel inflow. This reflects that the inflow over the Iceland-Faroe Ridge is not only dependent on the NAO-index, but also dependent on the position of the Icelandic low (Northern Center of Action, NCA, of the NAO; Hilmer and Jung, 2000). Comparing the two inflows through the Denmark Strait and the Faroe-Shetland Channel, gives a correlation coefficient of -0.54. This supports, to some degree, the observations which indicate that these two inflows are in counter-phase.

5.2 Svinøy Section

The Svinøy section is strategically placed across the core of the Norwegian Atlantic Current flowing northward along the Norwegian shelf, and has been monitored by moorings and frequent CTD-sections for several years. According to observations, the Norwegian Atlantic Current shows a two-branch structure, with one branch lying on the Norwegian shelf edge and the other branch located along the 2000 m isobath, following the topographic slope of the Vøring plateau, Orvik et al. (2001), Orvik & Niiler (2002).

5.2.1 Results

Figures 5.7 and 5.8 show the total and the Atlantic inflow through the Svinøy section. From the figures, it is clearly seen that both the total flow and the Atlantic inflow through the section have a large variability, both seasonally and interannually. The first observation is a clearly lower volume flux in the 1980s, until a sharp rise in the volume fluxes is seen in

1989. In the Atlantic layer, the lowest seasonal inflow is found during summer, with values of around 6 Sv. In October to January, the volume flux is increased to around 8 Sv, a difference of 25-30% of the flow. The seasonality in the total flow has a different phase, with the minimum flow in August and the maximum flow in March. On average, the model gives an Atlantic inflow of 7.0 Sv with a standard deviation of 1.8 Sv, while the total volume flux is 44.0 Sv with a standard deviation of 13.4 Sv. The large standard deviations reflect the large variabilities.

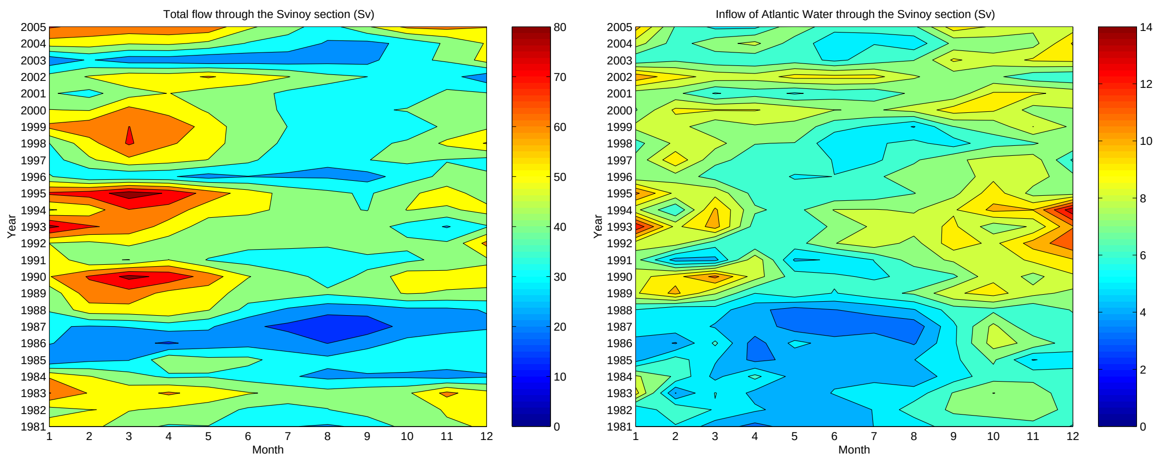

Figure 5.7: ***Total volume transport (left) and transport of Atlantic Water (right) through the Svinøy section.***

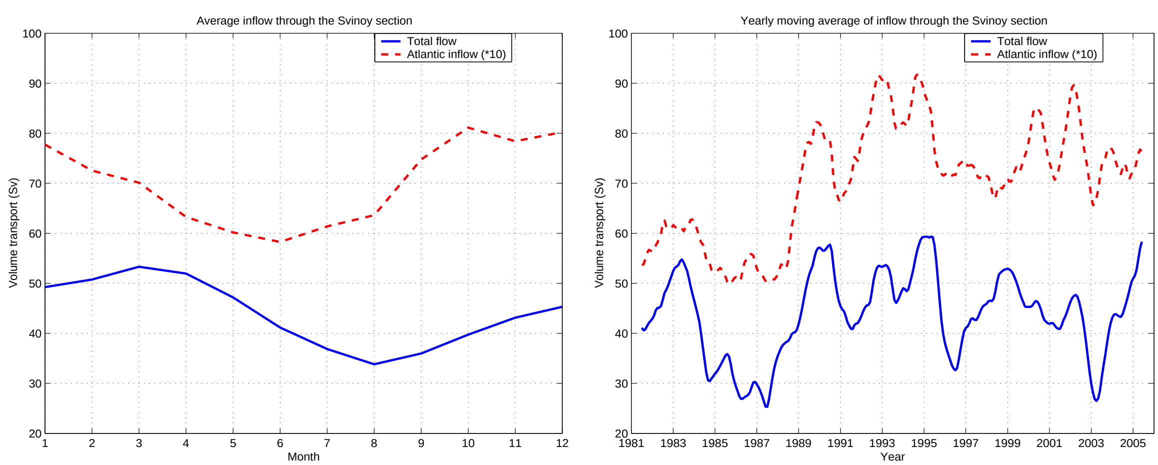

Figure 5.8: ***Volume fluxes through the Svinøy section. Note that the Atlantic inflow is multiplied by 10.***

To distinguish the two different branches in the Norwegian Atlantic Current, a vertical line has been drawn approximately at the 800 m isobath. The Atlantic inflow west of this line is hereafter termed "western branch" and the Atlantic inflow east of this line is termed "eastern branch". Inspection showed that this was an adequate choice for distinguishing the two branches. The inflow of Atlantic Water in the two branches is shown in figure 5.9. A striking observation is that the western branch seems to be almost non-existent from the start of the data set in 1981 until 1989. In 1989, it suddenly establishes and is consistent for the rest of the period (1989-2005). The eastern branch is well developed in all years. However, in the 1980s, the weak western branch is compensated by a slightly stronger eastern branch, although not enough to keep the total Atlantic inflow at the same level through the whole time series, as can be seen in figures 5.7 and 5.8. In the years 1981 to 1989, the western branch has an average volume transport of only 1.3 Sv, while the eastern branch has an average volume transport of 4.5 Sv. The standard deviations are 1.0 Sv and 1.2 Sv, respectively. The standard deviation is very high compared to the average in the western branch, reflecting that the western branch is both weak and highly variable in the 1980s. Figure 5.9 does not show any clear seasonal cycle in the western branch. However, it seems to be a higher inflow in summer and autumn than in winter and spring. This might be connected with summer heating at the surface, which is not excluded. Especially in the years with very low inflow, this may have a relatively strong influence on the calculated volume flux of Atlantic Water. Excluding the years 1981 to 1988 in the calculations, gives an average of 3.7 Sv in the western branch and 4.0 Sv in the eastern branch. The standard deviation is 1.2 Sv in both sections. Thus, the volume transport in the western branch is almost tripled, while the volume transport in the eastern branch has decreased slightly. It is also worth noting that while the total volume transport in the western branch is almost tripled, the standard deviation is the same, indicating a more consistent flow, or a consistent seasonal signal in all years.

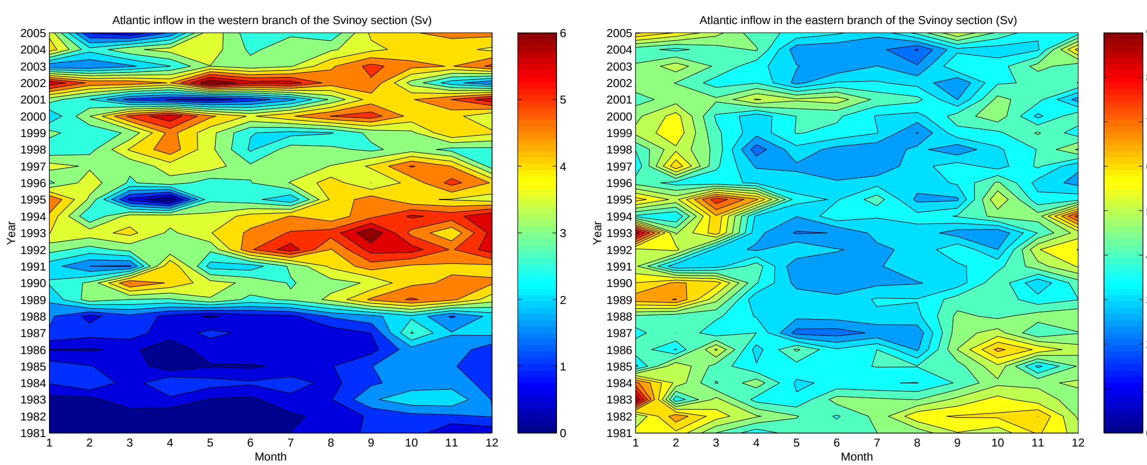

Figure 5.9: ***Volume transport of Atlantic Water in the western branch (left) and the eastern branch (right) of the Svinøy section.***

Looking at the velocity fields (figure 5.10), confirms that the western branch of the Norwegian Atlantic Current was almost absent in the 1980s. However, in 1995 there is a clear two branch structure, with the eastern branch following the continental slope, while the western branch follows the slope of the Vøring Plateau. This is also seen in the anomalies, with a negative anomaly of 0.1-0.15 m/s in the western branch in 1985, and a positive anomaly of 0.1 m/s in 1995. In the eastern branch, there is only small differences in both years. It is also clearly visible that the Atlantic inflow north of the Faroe Islands was weaker in the 1980s compared to the 1990s. Also the Shetland branch of the inflow show a positive anomaly in the current speed in the 1990s.

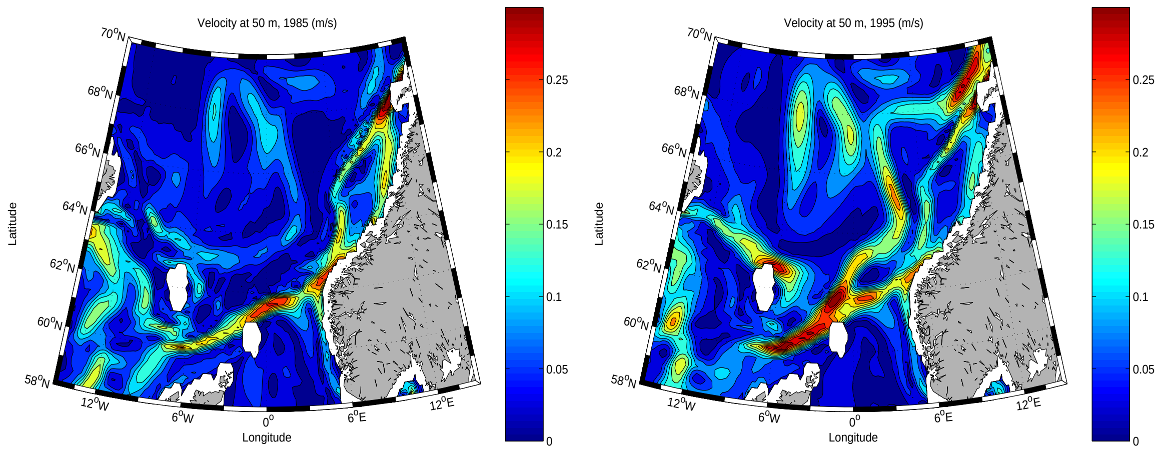

Figure 5.10: ***Yearly averaged velocities at 50 meter depth in 1985 (left) and 1995 (right). The color scale is the same in the two figures.***

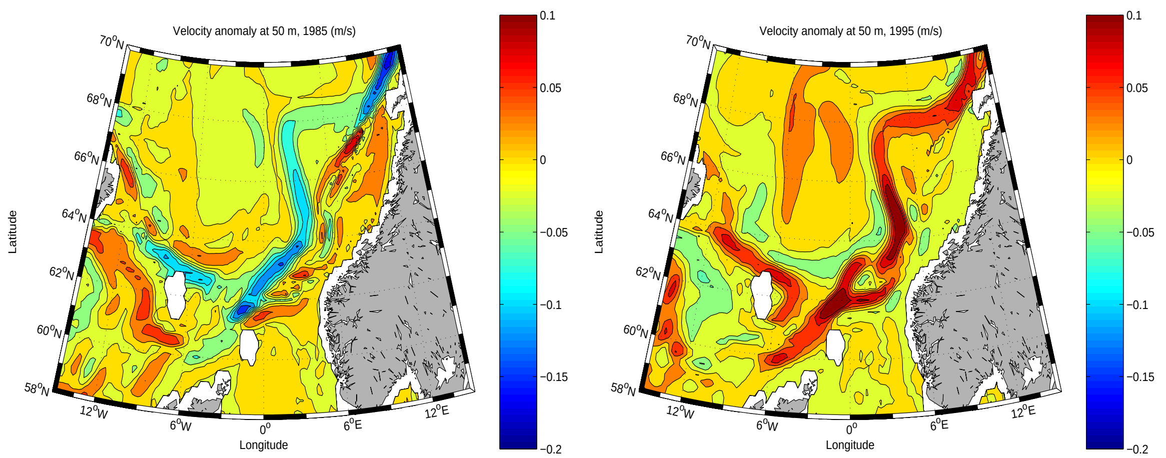

Figure 5.11: ***Yearly averaged velocity anomalies at 50 meter depth in 1985 (left) and 1995 (right). The color scale is the same in the two figures.***

Two parameters that affect both the volume transport and the heat flux, which will be discussed later, is the current speed through the section and the temperature across the section. Figure 5.12 shows the average temperature and the average current speed in the Atlantic layer through the Svinøy section. As can be seen, there is a clear seasonal signal in the average temperature, as expected. But the yearly average temperature is also oscillating, with a period of several years. This also seems to be the pattern in the average current speed, with the highest values in winter, but also large interannual variations. The highest values are found in January 1982, 1983 and 1993, with the monthly average current speed reaching 0.27-0.28 m/s.

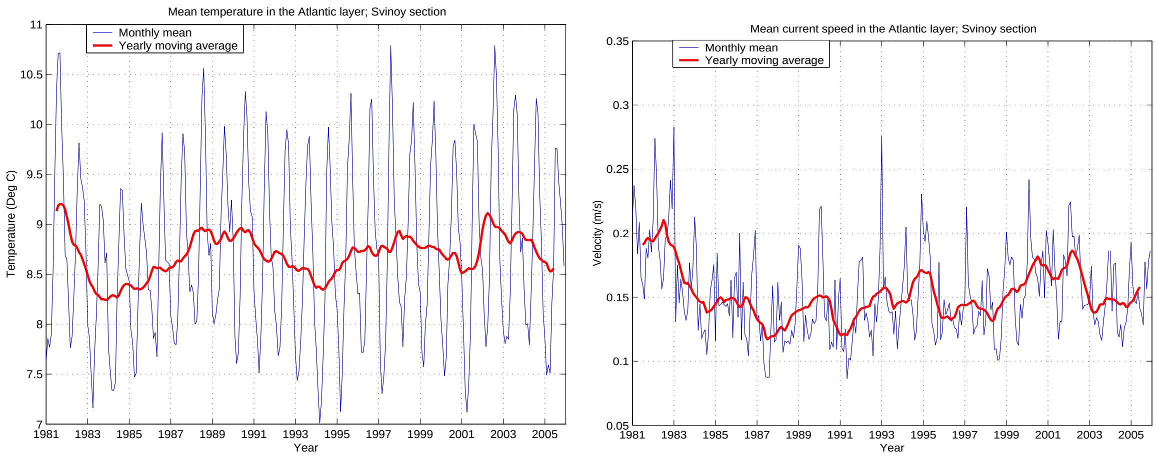

Figure 5.12: ***Average temperature (left) and current speed (right) in the Atlantic layer defined by temperature above 5 ^oC in the Svinøy section***

5.2.2 Discussion

The Svinøy section is strategically placed across the core of the Norwegian Atlantic Current, carrying Atlantic Water into the Nordic Seas. The Svinøy section monitoring program has been run since 1995, and time series of volume transports through the section stretching over several years are available. Based on four years of measurements (1995-1999) using both current meter moorings, VM-ADCP, SeaSoar-CTD and CTD transects, Orvik et al. (2001) estimated an inflow of 4.2 Sv in the eastern branch and 3.4 Sv in the western branch, with standard deviations of 1.5 Sv and 1.0 Sv, respectively. This gives a total Atlantic inflow of 7.6 Sv. This compares very well with the results found in the model, with an average volume transport of 2.8 Sv in the western branch and 4.2 Sv in the eastern branch, which gives a total Atlantic inflow of 7.0 Sv. These model results are based on the whole model period. However, it is more interesting to compare only the years when measurements are available. This will also cancel out the anomalously low inflow in the western branch during the 1980s. Including only the years 1995-1999, gives an average modeled volume transport of 3.4 Sv in the western branch and 3.8 Sv in the eastern branch; a total of 7.2 Sv. The standard deviations are 1.0 Sv and 1.2 Sv, respectively. Considering the relatively large uncertainties, these results are very close to the findings of Orvik et al. (2001).

Observations suggest that the inflow through the Faroe-Shetland Channel mainly feeds into the eastern branch of the Atlantic inflow, while the inflow between the Faroes and Greenland mainly feeds into the western branch (Orvik & Niiler 2002). Using monthly averages, gives a correlation coefficient of 0.57 between net Atlantic inflow through the Faroe-Shetland Channel and the volume transport in the eastern branch of the Norwegian Atlantic Current. Using the total Atlantic inflow through the Faroe-Shetland Channel gives a correlation coefficient of 0.73. Thus, the recirculation east of the Faroe Islands is also contributing to the flow in the eastern branch. On the other hand, there is only a weak and negative correlation between the volume transport in the western branch and the net Atlantic inflow west of the Faroe Islands (table 5.4). However, some of the Atlantic inflow recirculates in the Faroe-

Shetland Channel and subtracting this recirculation from the net Atlantic inflow between Greenland and the Faroes, gives a correlation coefficient of 0.31 between the net Atlantic inflow west of the Faroes and the western branch. This indicates that a high recirculation in the Faroe-Shetland Channel tends to weaken the western branch in the Svinøy section.

The two branches in the Norwegian Atlantic Current are believed to be in opposite phase (Mork & Blindheim 2000), and should thus be negatively correlated. This is consistent with observations showing opposite phases in the inflow through the Faroe-Shetland Channel and the inflow over the Iceland-Faroe Ridge. This is used to explain the rather stable inflow through the Svinøy section although the two branches in the inflow show a large variability. In the model, the monthly averages show a correlation of -0.23 between the two branches. Using yearly averages (July-June), gives a correlation of -0.49. Thus, the model supports the observed pattern of a negative correlation between the two branches, although the signal is rather weak. The correlations between the volume transports in different sections are summarized in table 5.4. Two interesting events show the negative correlation between the two branches clearly (figure 5.9). The first event occurs in March 1995, when there is an anomalously high inflow in the eastern branch. In the same month, there is almost a complete halt in the volume transport in the western branch. The second event occurs in winter and spring, 2001. Then there is another halt in the western branch inflow, from March to June. In the eastern branch, there is not any distinct high in the winter time inflow that year, but the seasonal high continues well into the summer (June/July). Except for the event with the stretching of the seasonal high in 2001, this phenomenon is only seen at the start of the time series, when the western branch is almost non-existent. Thus, when the western branch weakens, the volume transport in the eastern branch seems to increase to maintain the total volume transport through the Svinøy section.

Sections	Month	Winter
Greenland-Scotland Ridge - Svinøy Section (AW)	0.68	0.76
Faroe-Shetland Channel - Denmark Strait	-0.54	-0.84
Faroe-Shetland Channel - Eastern Branch	0.57	0.50
Iceland-Faroe Ridge+Denmark Strait - Western Branch	-0.18	-0.38
Faroe-Shetland Channel - NAO	0.36	0.40
Iceland-Faroe Ridge - NAO	0.28	0.49
Denmark Strait - NAO	-0.33	-0.40
Svinøy Section (AW) - NAO	0.35	0.46
Svinøy Section (Total) - NAO	0.27	0.46
Eastern Branch - NAO	0.45	0.64
Western Branch - NAO	0.06	0.14
Eastern Branch - Western Branch	-0.23	-0.07

Table 5.4: ***Correlations between the net Atlantic inflow through different sections. Winter is the months December-March.***

As can be seen in figure 5.2, the inflow through the Faroe-Shetland Channel was weak in the mid-1980s, while the inflow over the Iceland-Faroe Ridge was rather strong in the early 1980s. The low modeled volume transport in the western branch and the correspondingly higher volume transport in the eastern branch in the Svinøy section in the 1980s, contradict the observations suggesting that the Shetland-branch mainly feeds into the eastern branch and the inflow over the Iceland-Faroe Ridge mainly feeds into the western branch of the Norwegian Atlantic Current. However, figures 5.10 and 5.11 indicate that the inflow through the Faroe-Shetland Channel contributes to both branches in the 1990s, while this connection seems to be "shut" (at 50 meters) in the 1980s.

Table 5.5 shows the modeled and observed volume transports in the Svinøy section. There is very good agreement between model results and observations, but the modeled volume transport in the western branch is low compared to observations when the whole time series is used. The obvious reason for this is the already mentioned low inflow in the western branch during the 1980s.

	Modeled		Observations
Section	1981-2005	1995-1999	1995-1999
Western Branch	2.8	3.4	3.4
Eastern Branch	4.2	3.8	4.2
Total	7.0	7.2	7.6

Table 5.5: ***Modeled and observed Atlantic inflow through the Svinøy section. The observations are from Orvik et al, 2001.***

As can be seen from figures 5.7 and 5.8, the volume flux through the Svinøy section increases dramatically in the late 1980s. One factor that may trigger such large changes, is changes in the NAO. As can be seen from figure 5.5, the NAO-index increased and made a shift from negative to positive yearly values in 1988/89, and the winter values of the NAO-index shows a distinct peak in 1989. However, as the modeled volume flux through the Svinøy section and the NAO-index show only a weak correlation (table 5.4), the NAO seems insufficient to explain the dramatic shift in the volume transport. The event in January 1993 with the highest Atlantic inflow, is clearly connected with an increased average speed in the Norwegian Atlantic Current (figure 5.12). This is also the month when the Faroe-Shetland Channel experienced an extremely high inflow. However, there is nothing in the NAO-index that may explain this anomalous strong current.

Orvik et al. (2001) conclude that the eastern branch shows a systematic annual cycle with summer to winter variations in the proportion of 1 to 2. They also concluded that the volume transport in the flow correlated well with the NAO-index on a 3-month time scale. In the model, the seasonal signal is weaker, with a difference of 1 Sv, or almost 1/3 of the average flow, between summer and winter in the eastern branch. The western branch, on the other hand, shows no seasonal differences. Here, only the years 1995-1999 were used. Using 3-month averages of volume transport in the eastern branch and the NAO-index in these years, gives a correlation of 0.45, while the correlation between the volume transport in the eastern branch and net Atlantic inflow between Shetland and the Faroes is 0.86. Calculating seasonal differences for the whole model period, shows an average difference of 1.2 Sv between summer and winter values in the eastern branch, with the highest transports in winter. However, in 2001, the average volume transport was larger in summer. In the western branch, there is no evidence of any seasonal differences. One interesting observation is that in 2001, the western branch shows a considerably larger (1.2 Sv) volume transport in winter compared to the summer value that year. This coincides with the opposite seasonal difference in the eastern branch. The correlation between the seasonal differences in the two branches is -0.06.

Figure 5.8 reveals that the total flow and the Atlantic inflow through the Svinøy section have different phases. The Atlantic inflow, with a maximum in October to January, leads the total inflow, with a maximum in March, by a few months. This is also seen in the seasonal lows; the low in the Atlantic inflow occurs in June, while the low in the total flow occurs in August. This may suggest that the two have different forcing mechanisms. Based on monthly averages, the total flow and the Atlantic inflow have a correlation coefficient of 0.45. However, the highest correlation is found by comparing the Atlantic flow with the total flow one or two months later, which both gives a correlation of 0.56.

A strong correlation between the total inflow over the Greenland-Scotland Ridge and the Atlantic inflow through the Svinøy section is to be expected. Correlation coefficients for different time spans are shown in table 5.4. Using monthly averages gives a correlation coefficient of 0.68. However, 0.68 is is not a very high correlation, which is indicating that other factors contribute to the variability in the Svinøy section. Using winter values (December-March) gives a correlation of 0.76.

As shown in both figures 5.7 and 5.8, the Norwegian Atlantic Current shows a high variability, both on yearly and monthly timescales. Using monthly averages, gives a correlation coefficient of 0.35 between the Atlantic inflow in the Svinøy section and the NAO-index, while using winter values only gives a correlation coefficient of 0.46. The two branches of the Atlantic inflow show different responses to the NAO. While the eastern branch is dependent of the NAO, to some degree, the western branch shows no connection to shifts in the NAO. This is consistent with the findings of Orvik et al. (2001), concluding that the eastern branch is a topographically trapped and near barotropic current, while the western branch appears as an unstable frontal jet.

Chapter 6

Outflow over the Greenland-Scotland Ridge

The inflow of Atlantic Water into the Nordic Seas is compensated by an outflow of deep water over the Greenland-Scotland Ridge and also a southward transport of cold surface and intermediate water and ice through the Denmark Strait. In this chapter, the outflow of water masses with temperatures below 5 ^{o}C over the Greenland-Scotland Ridge, will be presented.

6.1 Results

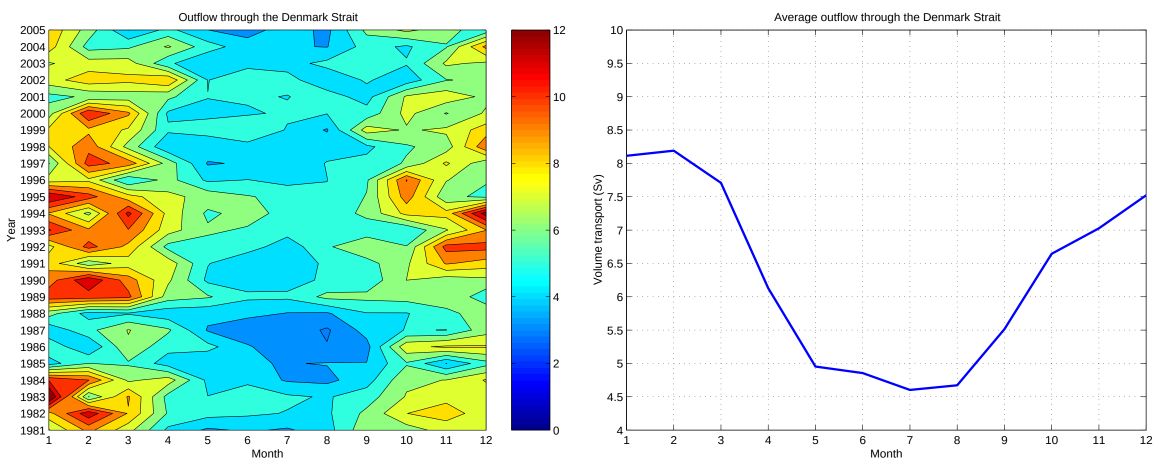

Figure 6.1: ***Outflow through the Denmark Strait.***

The main contributor to the outflow from the Nordic Seas to the Atlantic is the Denmark Strait. Some of the volume transport through this section is by southward advection of ice along the eastern coast of Greenland. However, ice-transport will not be studied in this work. In the model, an average of 6.4 Sv is transported out of the Nordic Seas through the Denmark Strait. As can be seen in figure 6.1, there is a clear seasonal cycle in the Denmark Strait outflow, with the highest transport in winter. The ratio between summer and winter values is almost 1 to 2, with just above 8 Sv in winter and below 5 Sv in summer, on average. However, there are also some interannual changes in the outflow. As can be seen in figure 6.1, the outflow was substantially lower during parts of the 1980s, especially in winter.

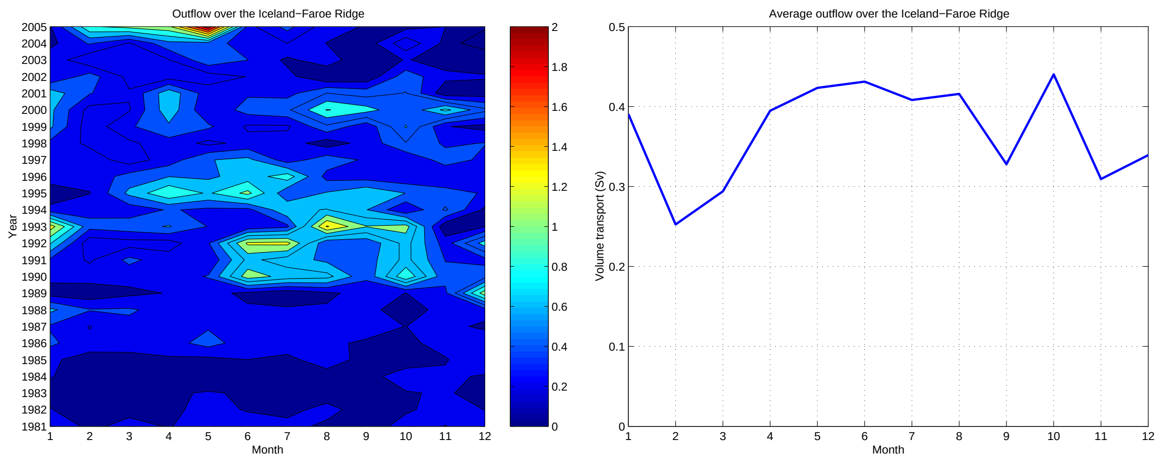

Figure 6.2: ***Outflow over the Iceland-Faroe Ridge.***

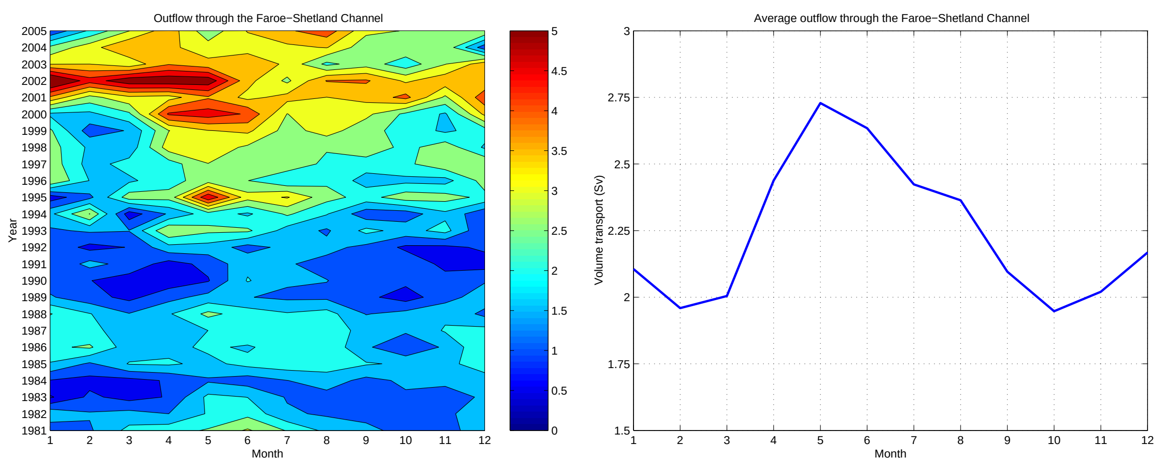

Figure 6.3: ***Outflow through the Faroe-Shetland Channel.***

Figures 6.2 and 6.3 show the outflow through the Iceland-Faroe section and the Faroe-Shetland Channel, respectively. The figures show that in both sections, the interannual variations are larger than seasonal variations. In the Faroe-Shetland Channel, there is clearly a larger outflow in the second half of the modeled period, compared to the first half. Including the whole time series gives an average outflow of 2.2 Sv through this section. Over the Iceland-Faroe Ridge, the situation is different, with the largest outflow in the years around 1990, and lower outflow at the start and at the end of the modeled period. On average, only 0.4 Sv leaves the Nordic Seas through this section. Note that these numbers only include water masses with temperatures below 5 ^{o}C.

6.2 Discussion

The total outflow, which includes both the recirculating Atlantic Water and the outflow of water masses with temperatures below 5 ^{o}C in the three sections, are shown in table 6.1. More than half the outflow through the Faroe-Shetland Channel is outflow of Atlantic Water either due to recirculation or eddy-acticity in the section. On the Iceland-Faroe Ridge, the Atlantic Water accounts for around two thirds of the outflow. In the Denmark Strait, the situation is totally different, with very little recirculation of Atlantic Water.

	ROMS			
Sections	Total	Below 5 degC	Observations	MICOM
Faroe-Shetland Channel	4.9	2.2	4.5 (2.6)	2.1
Iceland-Faroe Ridge	1.4	0.4	1.0	3.6
Denmark Strait	6.4	6.3	4.3	4.3

Table 6.1: ***Southward volume transports over the Greenland-Scotland Ridge. Observations are from Hansen and Østerhus, 2000 and the model results from MICOM are from Nilsen et al, 2003. The number in parantheses is the deep waters alone, which should be close to the total outflow corrected for recirculation of Atlantic Water.***

Table 6.2 shows correlations between the outflow in different sections and the NAO-index. The table shows values for the total outflow, while the numbers in paranthesis show values when the Atlantic Water is excluded. There is a high, negative correlation between the total outflow through the Faroe-Shetland Channel and the total outflow between Greenland and the Faroes. Generally, the correlations based on the outflow of water colder than 5 ^{o}C are considerably lower than the correspondingly correlations where also the Atlantic Water is included. Figure 6.4 shows the yearly moving averages of the total outflow (including Atlantic Water) in the Faroe-Shetland Channel and between Greenland and the Faroes.

Sections	Monthly	Winter
Faroe-Shetland Channel - Greenland-Faroe	-0.57 (-0.32)	-0.76 (-0.46)
Faroe-Shetland Channel - Denmark Strait	-0.49 (-0.33)	-0.70 (-0.45)
Faroe-Shetland Channel - NAO	-0.33 (-0.23)	-0.62 (-0.52)
Iceland-Faroe Ridge - NAO	-0.09 (-0.14)	0.21 (-0.07)
Denmark Strait - NAO	0.52 (0.51)	0.79 (0.77)

Table 6.2: ***Correlations between the total outflow through different sections and also compared to the NAO index. Values in paranthesis are with the Atlantic Water excluded.***

The most distinct current in the Denmark Strait is the southward surface flow of cold water (not shown). Figure 6.1 shows that the Denmark Strait outflow is variable, and that there is a clear seasonal signal in the outflow. The largest outflow ocurrs during winter (Oc-

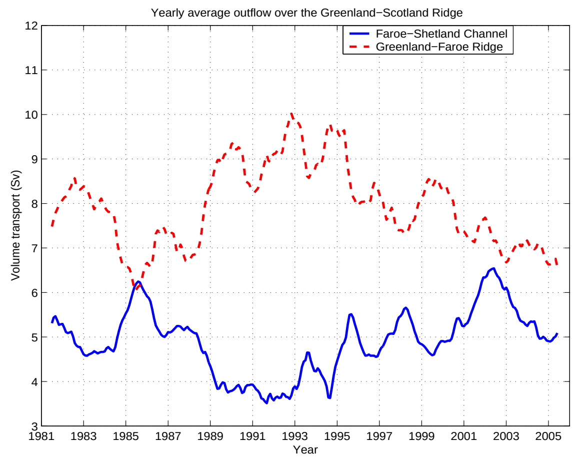

Figure 6.4: ***Yearly moving averages of total outflow through the Faroe-Shetland Channel and between Greenland and the Faroes.***

tober through March), with seasonal differences of around 3.5 Sv. This contradicts existing literature, e.g. Dickson & Brown (1994), who found no significant seasonal cycle in the Denmark Strait overflow. However, outflow at all levels are included in this study. A separation into upper, intermediate and deep waters, may give a different picture of the seasonal and interannual variability. The yearly seasonality and the seasonal mean show a correlation of 0.75, with no values below 0.5. This indicates a consistent seasonal pattern of the flow. The years 1985 through 1988 differ from other years (figure 6.1). In these years, the outflow is lower compared to other years, and the signal is seen throughout the year, and this contribute to the large year to year variations. Macrander et al. (2005) argue that the lack of interannual variability in earlier measurements, are due to the lack of continous long time-series. From measurement data obtained over a period of 4 years, they conclude that the Denmark Strait overflow is larger than earlier observed, and is varying by as much as 20%, from 3.0 Sv to 3.7 Sv, while earlier observations indicated a more stable flow of 2.7-2.9 Sv. This interannually variability is supported by these model results. Macrander et al. (2005) do not mention any strong seasonality in the Denmark Strait overflow. However, only volume transports below the layer of maximum current shear was included. Thus, the results from the model, including both deep water and surface water, is expected to give higher volume transports than the estimates based on observations.

Nilsen et al. (2003) found a southward transport of 4.3 Sv through the Denmark Strait, using the isopycnic ocean model MICOM. This result compared well with existing literature. Hansen & Østerhus (2000) estimated an outflow of 6.0 Sv through the Denmark Strait and the Canadian Archipelago. Fissel et al. (1988) estimated the transport through the Canadian Archipelago to be 1.7 Sv, which leaves 4.3 Sv to be transported through the Denmark Strait. Compared to these results, the transport obtained in this model study is quite high. These model results also indicate that there is no net volume transport through the Canadian Archipelago. However, the Canadian Archipelago is not included in this work, and the question is therefore left without any thorough answers.

A substantial part of the outflow through the two other sections on the G-S Ridge, is recirculation of Atlantic Water, mainly in the Faroe-Shetland Channel. Compared to observations, the model is quite close in reproducing the outflow through the Faroe-Shetland Channel, both with respect to the recirculated Atlantic Water and the colder water masses alone. The total outflow of 4.9 Sv agrees well with the total outflow of 4.5 Sv found by Hansen & Østerhus (2000). Subtracting the Atlantic Water component, gives an outflow of 2.2 Sv of colder water masses, which is consistent with the deep water outflow of 2.6 Sv reported from observations. The outflow over the Iceland-Faroe Ridge, compares less well with observations, with 1.1 Sv Atlantic Water and only 0.4 Sv of colder water masses. However, this indicates a lot of eddy-activity on the ridge, which may give measurements a large variability and uncertainty. Nilsen et al. (2003) found a very large outflow, but also a very large inflow through this section in their model study. However, they concluded that the net inflow was close to observations. In these model results, a total inflow of 4.4 Sv and a total outflow of 1.5 Sv gives a net inflow of 2.9 Sv through the section, which is relatively close to the 2.3 Sv net inflow found by Hansen & Østerhus (2000).

The main difference between the inflow and the outflow in the two sections, is the lack of any seasonal cycle in the outflow. On the other hand, the outflow in both sections show a large interannual variation. This interannual variability is different in the two sections. The outflow between the Faroes and Shetland show a significant increase throughout the modeled period. Generally, the highest values are found in spring/early summer. On the Iceland-Faroe Ridge, there is a substantially larger outflow through some years in early and mid-1990s. These highs mainly ocurrs in summer. However, towards the end of the modeled period, the outflow returns to the values found in the 1980s. Note also the maximum outflow in January 1993, which coincides with the maximum Atlantic inflow through the Faroe-Shetland Channel (figure 5.2). The reason for this high is not known, but the same explanation as for the record high Atlantic inflow in the Faroe-Shetland Channel in the same month is suggested; that this is due to extreme low pressure activity in the region, that is not captured in the NAO-index.

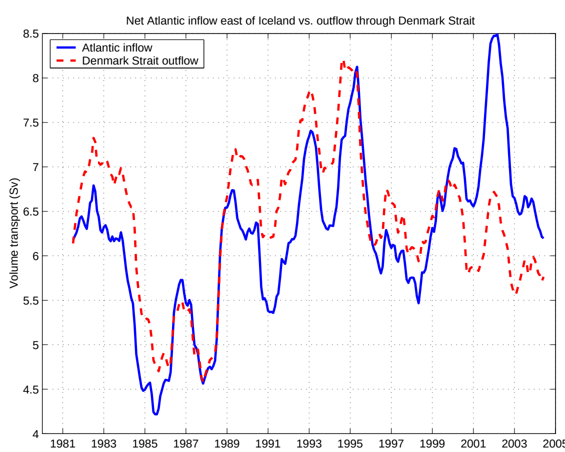

Figure 6.5: ***Yearly moving averages of net Atlantic inflow between Iceland and Scotland and outflow of water masses with temperatures below 5 ^oC in the Denmark Strait.***

Using monthly averages, the correlation between the total outflow through the Faroe-Shetland Channel and the total outflow between Greenland and the Faroes was found to be -0.57. Using winter values only gives a correlation of -0.76 (see figure 6.4 and table 6.2). The corresponding correlations between the Faroe-Shetland Channel and the Denmark Strait are -0.49 and -0.70, respectively. Thus, the total outflow between the Faroes and Greenland is in counter-phase with the outflow through the Faroe-Shetland Channel. The correlation between the net Atlantic inflow over the Greenland-Scotland Ridge and the outflow of water masses with temperatures below 5 ^{o}C through the Denmark Strait is found to be 0.85, while including only the Atlantic inflow east of Iceland gives a correlation of 0.83. Thus, there seems to be a close connection between the Atlantic inflow into the Nordic Seas and the outflow of cold water masses through the Denmark Strait (figure 6.5). Calculating the correlation between outflow through the Denmark Strait and the NAO-index, reveales a correlation of 0.52 using monthly means and 0.79 using winter values. In the other two sections, a correlation of -0.62 was found between the NAO-index and the total outflow through the Faroe-Shetland Channel, using winter values only. Ignoring the Atlantic Water component of the outflow reduces the correlation to -0.52. For the Iceland-Faroe section, the correlations between outflow and NOA-index are insignificant. This implies that the outflow over the Iceland-Faroe Ridge is the section which is less sensitive to changes in the NAO. This is also expected, as a high NAO-index will allow more water to leave the Nordic Seas through the Denmark Strait (especially in upper layers, where the East Greenland Current is both strong and highly variable). A high NAO-index will also block for some of the outflow through the Faroe-Shetland Channel. The low correlation between the NAO-index and the outflow over the Iceland-Faroe Ridge, may again be explained by the variability of the Northern Center of Action (NCA); the variability in the position of the Icelandic low. The higher correlation between the NAO-index and the total outflow over the Greenland-Scotland Ridge, compared to only the outflow of colder water masses, may be explained by that the Atlantic Water is found in upper layers while the colder water is found in deeper layers, except for the cold surface water in the Denmark Strait. Thus, the colder water masses are less sensitive to wind forcing.

Chapter 7

Arctic exchange

The exchange between the Atlantic and the Arctic Ocean plays an important role in the thermohaline circulation in the world oceans. The Arctic is connected to the world oceans through the Bering Strait, the Canadian Archipelago and through the Nordic Seas. The connection through the Nordic Seas differ greatly from the other two, due to the inflow of warm Atlantic Water through the Nordic Seas, giving a net heat loss to the atmosphere in both the Nordic Seas and in the Arctic, see e.g. Simonsen & Haugan (1996). Atlantic Water enters the Arctic Ocean both through the Fram Strait and through he Barents Sea, and cold Arctic Water is transported out of the Arctic (figure 4.1). Changes in the inflow or in the heat content in the Atlantic Water entering the Arctic Ocean, may have a large impact on the climate in Polar regions (see e.g. the ACIA-report on impacts of a warming Arctic). A warming of the Atlantic Water layer in the Arctic in the early 1990s is reported, with the average temperature rising by as much as 1 ^{o}C, Grotefendt et al. (1998) and Quadfasel et al. (1991). In this section, the water mass exchanges between the Nordic Seas and the Arctic Ocean will be investigated in some detail, with main focus on the Fram Strait.

7.1 Fram Strait

The Fram Strait is an area of large interest because a large portion of the exchange of Arctic Water and Atlantic Water between the Arctic Ocean and the Atlantic takes place through this passage. There is also a large transport of sea-ice out of the Arctic through the Fram Strait, but ice-transport is not studied in this work.

7.1.1 Results

The modeled volume fluxes through the Fram Strait are shown in figure 7.1. On average, the model gives a total northward volume flux of 9.0 Sv with a standard deviation of 4.1 Sv. Southward, the volume flux is 13.6 Sv with a standard deviation of 5.0 Sv. The relatively large standard deviations are clearly due to the large seasonal and interannual variability of both the inflow and the outflow. A maximum is found in the flow in both directions in late winter/early spring and a minimum is found during summer. Computing summer and winter averages gives an average southward flow of 11.6 Sv in summer and 15.4 Sv in winter. The numbers for the northward flow are 8.0 Sv and 9.8 Sv, respectively.

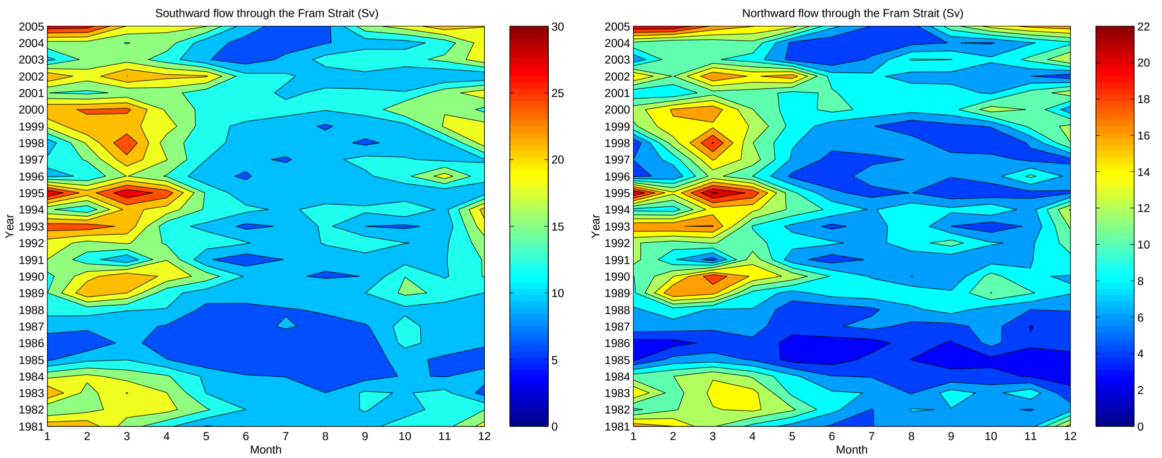

Figure 7.1: ***Southward (left) and northward (right) volume transports through the Fram Strait.***

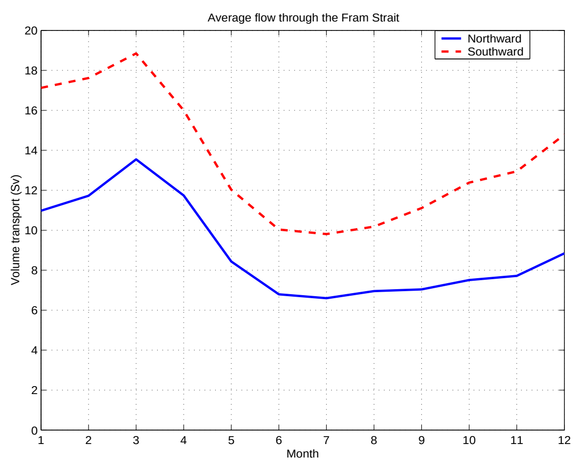

Figure 7.2: ***Seasonal volume fluxes through the Fram Strait.***

Figure 7.3 shows the mean temperature in the northward and southward flowing water masses in the Fram Strait. A large variability in the northward temperature is revealed, while the temperature in the southward flowing water masses seems to have a trend towards a higher temperature. The yearly running mean of the temperature in the northward flowing water masses is varying with almost 1 ^{o}C, from 0.3 ^{o}C in the mid-1980s to almost 1.3 ^{o}C in 1990. There is also a clear seasonal cycle in the temperatures, with the highest temperatures in autumn. However, surface water is not filtered out, and is contributing to higher temperatures in autumn. The mean current speeds (figure 7.4) show a more similar pattern in both directions than temperature, with a distinct low in the mid-1980s. Typically, the highest values of the average current speed is found in winter, with values between 0.05 and 0.1 m/s,

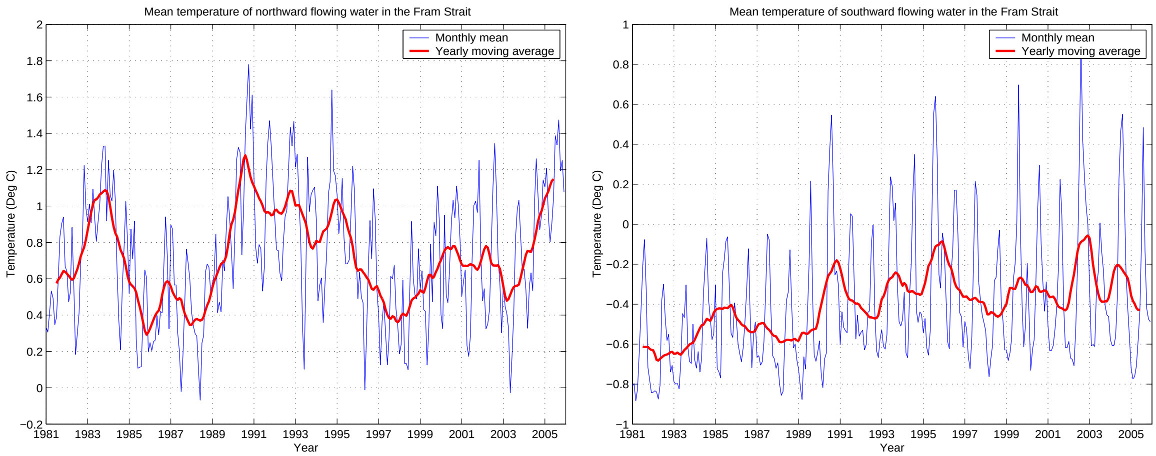

Figure 7.3: ***Mean temperature of northward flowing water (left) and southward flowing water (right) in the Fram Strait.***

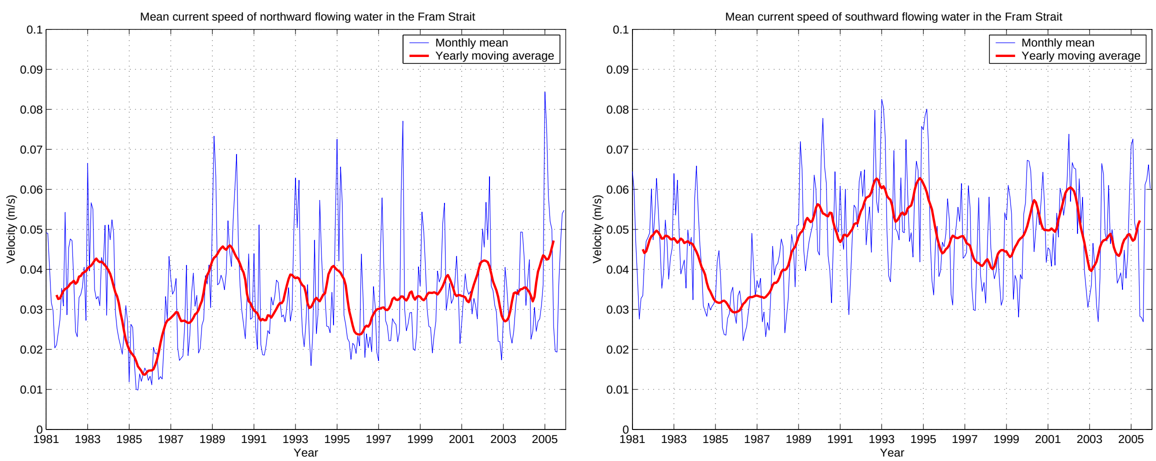

Figure 7.4: ***Mean current speed of northward flowing water (left) and southward flowing water (right) in the Fram Strait.***

while summer values are generally below 0.03 m/s in the northward flow and 0.04 m/s in the southward flow.

7.1.2 Discussion

The volume transports found in the model are in good agreement with the findings of Schauer et al. (2004), estimating a total northward transport between 9 and 10 Sv, with standard deviations of 2 and 1 Sv, respectively. The southward volume transport was found to be between 12 and 13 Sv, with standard deviations of 1 and 2 Sv, respectively. Schauer et al. (2004) used a section consisting of 14 moorings along 78^o55'N, stretching from 6^o51'W on the Greenland shelf break to 8^o40'E on the western shelf break off Spitsbergen, thus only slightly south of the modeled section presented in this study. Fahrbach et al. (2001) estimated a northward volume transport of 9.5 Sv in the Fram Strait, with a standard deviation of 1.4

Sv. A southward volume transport of 11.1 Sv was estimated, with a corresponding standard deviation of 1.7 Sv. Overall, they found a net southward transport of 4.2 Sv +/- 2.3 Sv. The results of Schauer et al. (2004) were based on 3 years of measurements, from September 1997 to July 2000. Calculating the modeled volume transports during this period, gives a southward transport of 15.3 Sv and a northward transport of 9.7 Sv. These transports are slightly higher than the average transports for the whole time series. There is a clear seasonal cycle in both the inflow and the outflow in the model. By direct observations, Schauer et al. (2004) and Fahrbach et al. (2001) found that the northward flow through the section is strongest in winter, while the southward flow of volume and heat did not show any clear seasonal signal.

Figure 7.4 shows that the reduced flow in the mid-1980s is due to lower current speeds through the section. Lower temperatures in the same period also contribute to reduced volume transport of water with Atlantic origin. It seems to be the lack of a winter maximum in the years 1985 and 1986 that is the main reason for the drastically reduced volume transports in those two years. However, although also the summer values was below average, the largest anomalies are seen in winter. In 1986, the average current speed rises sharply, and is returned to "normal" values by 1990. From 1988 to 1991, the average temperature in the northward flowing water rises dramatically, from 0.4 ^{o}C to 1 ^{o}C in the yearly moving average. However, fluctuations in both average temperature and average current speed are also seen later in the time series. The increased inflow of water originating from the Atlantic, is in agreement with the findings of Dickson et al. (2000), who concluded that the Arctic warming in the early 1990s probably was a combination of both warmer and stronger inflow of Atlantic Water. According to Dickson et al. (2000), this might be due to increased NAO index and advection of atmospheric heat into the Nordic Seas, reducing the oceanic heat loss in the Nordic Seas. The heat transport through Fram Strait and other sections is discussed in a later chapter.

7.2 Barents Sea Opening

The modeled exchange between the Barents and the Nordic Seas is already done by Budgell (2005). Here, only a brief presentation of these results is given. In this model run, a total of 4.3 Sv is flowing into the Barents. With 1 Sv leaving the Barents through the Fugløya-Bjørnøya section, a net inflow of 3.3 Sv is found. This agrees with the findings of Budgell (2005), even though he used a grid with a horizontal resolution of about 9 km, compared to about 20 km in this model run. These transports are high compared to observations; based on fixed current meter mooring arrays, Ingvaldsen et al. (2004) estimated a net Atlantic inflow of 1.5 Sv into the Barents. Model studies by Maslowski et al. (2004) showed a net volume transport of 3.3 Sv (2.5 Sv Atlantic Water) into the Barents when the section was stretched to include the whole Barents entrance between Norway and Spitsbergen. Including the part of the section north of Bjørnøya, a net flow of 3.4 Sv into the Barents is found in this model run. However, these model results include the Norwegian Coastal Current (NCC), which may contribute with as much as 1 Sv. Due to the poor salinity fields in this model run, the NCC can not be separated from Atlantic water masses.

Chapter 8

Volume transports through the Nordic Seas

After the investigation of all the sections closing the Nordic Seas basin, an estimate of the total volume flux through the Nordic Seas can be made (see figure 4.3). All water masses entering the Nordic Seas are defined as "inflow" and all water masses leaving the Nordic Seas are defined as "outflow". Inflow, outflow and net volume fluxes through the different sections are shown in table 8.1. On average, a total of 23.2 Sv is flowing into the Nordic Seas basin and 23.8 Sv is leaving the basin, which gives a net outflow of 0.6 Sv. This offset of about 3% is considered acceptable, taken into account the uncertainties in the volume fluxes through the different sections, the coarse model resolution and also that there might be some small leakage between the sections.

By the use of existing literature, an estimate of the total volume flux through the Nordic Seas based on observations, is made. However, due to the lack of available data, this estimate is not complete. The main contributors are, however, present. Both the inflow over the G-S Ridge and the exchanges through the Fram Strait are subjected to several investigations. Some of the observations are summarized in table 8.1. Ingvaldsen et al. (2004) estimated a net Atlantic inflow of 1.5 Sv through the Barents Sea Opening. The other entrance to the Barents Sea, between the Bjørnøya and Spitsbergen, accounts only for a minor part of the exchange between the Norwegian Sea and the Barents Sea. The other uncertain section is the Utsira West section, which covers the entrance from the Norwegian Sea into the North Sea. As this is the only entrance to the North Sea, except for the British Channel, the northward and southward flux through the Utsira West section must balance (the exchange through the British Channel is only minor). The North Sea is, like the Barents Sea, a shallow sea, which means that the currents are mainly wind-driven. As shown for the Barents Sea, the model gives too high values for the flow in shallow areas. Whether or not this also applies for the North Sea is unknown. However, the net flow through the Utsira West section should be close to zero.

A close inspection shows that the outflow over the G-S Ridge exceeds the inflow by 1.8 Sv. However, water masses with temperatures below 5 ^{o}C entering the Nordic Seas through the Denmark Strait, are not accounted for. This amounts to 0.8 Sv (note the total inflow of

1.6 Sv compared to the Atlantic inflow of 0.8 Sv). The remaining 1 Sv is from the 1 Sv that is put into the model through the Bering Strait and removed along the southern boundary. However, this leaves the flux through the Canadian Archipelago to balance, which contradicts observations suggesting that there is a net southward flow of 1.7 Sv through the archipelago (Fissel et al. 1988).

	Model			Observations		
Section	Inflow	Outflow	Netflow	inflow	outflow	netflow
Denmark Strait	0.8 - 0.3	6.3 - 1.9	-5.5	1.0	4.3	-3.3
Iceland-Faroe	3.0 - 1.0	0.4 - 0.3	2.6	3.3	1.0	2.3
Faroe-Orkney	3.2 - 1.5	2.2 - 1.0	1.0	4.3	2.6	1.7
Utsira-Orkney	1.2 - 0.5	1.1 - 0.4	0.1			
Fugløya-Bjørnøya	1.0 - 0.4	4.3 - 1.1	-3.3		1.5*	-1.5*
Bjørnøya-Spitsbergen	0.4 - 0.2	0.5 - 0.2	-0.1			
Fram Strait	13.6 - 5.0	9.0 - 4.1	4.6	12-13 - 2	9-10 - 2	2-4 - 2
Total	23.2	23.8	-0.6	21.1	18.9	2.2

Table 8.1: ***Volume fluxes through the sections closing the Nordic Seas, with standard deviations. *Atlantic Water only.***

Chapter 9

East Greenland Current

The East Greenland Current carries cold water originating from the Arctic southward from the Fram Strait to the Denmark Strait and into the Atlantic Ocean. The current also carries some Atlantic Water that is recirculated in the Fram Strait and therefore never enters the Arctic Ocean. A considerable amount of freshwater in the form of sea-ice is also transported southward by this current. In order to capture the volume transport in the East Greenland Current, a section stretching from the eastern coast of Greenland, at 75^oN and eastward to the 8^oW-meridian, at 74^oN, has been used to study the temperature and volume transport.

9.1 Results

The total volume transport in the East Greenland Current is shown in figure 9.1. A clear seasonality in the flow is revealed, but also a remarkably high interannual variability. Especially two distinct extremes are seen. A very low volume transport is evident in the mid-1980s, with the yearly mean dropping below 10 Sv and monthly means as low as 2.3 Sv and 2.5 Sv in July 1985 and 1987, respectively. The other extreme is the maximum volume transport in 1995, reaching 55.9 Sv in January and the yearly mean exceeding 30 Sv. Averaged over the whole time series, the model shows a volume transport of 20.5 Sv with a standard deviation of 9.7 Sv. The high standard deviation, 50 % of the average flow, reflects the very large variability in the volume transport.

Figure 9.1 shows a clear seasonal cycle in the East Greenland Current, with the largest transport found in winter and a considerably smaller transport in summer. This is also in accordance with the total flow through the Svinøy section (figure 5.7) and the flow through the Fram Strait (figure 7.1) and the outflow through the Denmark Strait (figure 6.1).

9.2 Discussion

The average volume transport in the East Greenland Current found in the model, is remarkably close to the findings of Woodgate et al. (1999). Based on direct current measurements, they found an average volume transport of 21 Sv +/- 3 Sv. However, they pointed out that it is difficult to locate the eastern edge of the current, and therefore, they calculated the av-

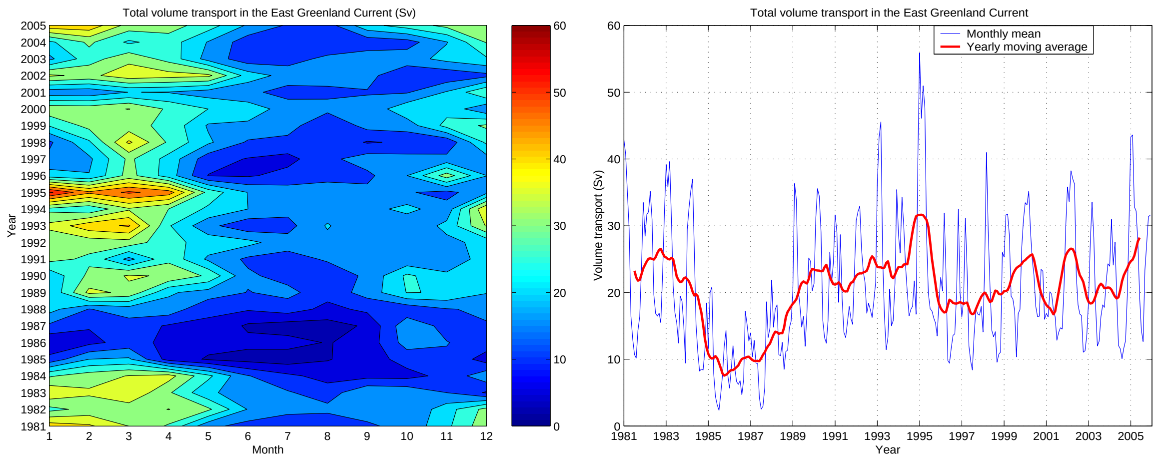

Figure 9.1: ***Total volume transport in the East Greenland Current.***

erage volume transport using different moorings. Using the moorings extending from 14^{o}W to 10^{o}W gives an average transport of 16 Sv, while including the mooring at approximately 8^{o}W gave a transport of 25 Sv. However, their best estimate is a section from 14^{o}W to 9^{o}W, which gives an average transport of 21 Sv. Using the model data, gives a yearly average transport of 31.6 Sv in the period July 1994 to June 1995, which is 20 % larger than the 25 Sv observed when using the maximum range of the moorings, east to 8^{o}W. Woodgate et al. (1999) also found a clear seasonal signal, with a minimum monthly transport of 11 Sv in summer and a maximum monthly transport of 37 Sv in winter, both with errors on the order of 5 Sv. These observations were based on the best estimate, east to 9^{o}W. In the model, the winter maximum is found i March, with an average volume transport of 31 Sv, while the minimum in summer is found in July/August, with an average volume transport of 13 Sv. The standard deviations are 10 Sv and 5 Sv, respectively. Using the total range of the measurements, showed a seasonal cycle ranging from 14 Sv in summer to 41 Sv in winter. Calculating corresponding values from the model (1994/1995) gives the values 17 Sv in summer and 56 Sv in winter. Thus, it is worth noting that Woodgate et al. (1999) deployed their moorings in the year when the model shows the largest volume transport in the whole 25 year period the model is run. Measurements from earlier years indicate that the current has low interannual variability (Woodgate et al. 1999). This is contradicted by the model results, showing a large year to year variability (figure 9.1). The high variability is reflected in the high standard deviation, which is as large as 50% of the mean flow. The high seasonal variability reported by Woodgate et al. (1999), contradicts previous literature stating that no seasonal or interannual variability is found in the southward flow through the Fram Strait (Foldvik et al. 1988) or in the Denmark Strait overflow (Dickson & Brown 1994). However, based on recent measurements, Macrander et al. (2005) show that interannual variability is present in the Denmark Strait overflow, and that previous estimates of the Denmark Strait overflow may be too low. As seen earlier, the model results do indeed show great variability, both seasonally and interannually in the Fram and Denmark Straits and in the East Greenland Current.

	Models				Observations	
Water mass	ROMS	S 91	L 91	F 95	W 99	F 95
All	20.5	19	13.6	12	21	25
Atlantic Water	7.7				8	
Seasonal range	13-31	13-31			11-37	

Table 9.1: ***Volume transports in the East Greenland Current. Sources are: S 91 - Stevens, 1991; L 91 - Legutke, 1991; F 95 - Fahrbach et al, 1995; W 99 - Woodgate et al, 1999.***

9.3 Recirculated Atlantic Water

In the East Greenland Current, water of Atlantic origin, hereafter termed recirculated Atlantic Water, is easily distinguishable as a core of warmer water flowing southward along the shelf slope of Greenland, while the upper layer part of the East Greenland Current is seen as a strong and narrow current on the Greenland shelf, transporting cold surface water southwards. To quantify the flux of recirculated Atlantic Water, I have calculated the southward transport of water with temperatures above 0 ^{o}C. The recirculated Atlantic Water is isolated from the surface by a cold surface layer most of the year. However, during summer, the surface layer is heated and the highest temperatures are found in the upper 50 meters. To filter out this “noise” of warm summer water at the surface, where the strongest currents are found, I have canceled out all water masses in the upper 30 meters when looking at recirculated Atlantic Water. The volume flux of recirculated Atlantic Water is shown in figure 9.2. As can be seen in the figure, the flow is highly variable, and shows the same features as the total volume flux in the East Greenland Current. At the start of the time series, a remarkably high flow is seen, reaching 20.2 Sv in February 1981. However, as this is very early in the time series, this might be due to some spin-up effects and the results should not be fully trusted. In the mid-1980s, the flow almost ceased totally, with the monthly averages dropping to 0.6 Sv in July 1985 and 0.2 Sv in July 1987. At this time, the dynamics in the model should be in balance, thus, this low not only seen in the East Greenland Current, but in the whole Nordic Seas basin, is supposed to reflect reality. In 1995 another high is seen, reaching 20.6 Sv in March, with the yearly running mean reaching 12.1 Sv. The peak in 1995 may be in association with the higher Atlantic inflow through the Svinøy section during the winters 92/93 and 94/95 (figures 5.7 and 5.8). The high volume transport of recirculated Atlantic Water in 1995 coincides with the extremely large volume transport in the East Greenland Current in winter 1995 (figure 9.1). This may imply that more recirculated Atlantic Water is formed by mixing with other water masses in winter 1994/1995, and also a larger flow from the Arctic through the Fram Strait, see figure 7.1. However, the largest flux of recirculated Atlantic Water takes place in February 2005, when the volume transport reaches 20.8 Sv. Looking at figure 9.3, reveals that the high in winter 1981 is mostly due to higher temperatures or a larger body of recirculated Atlantic Water in 1981, as the current speed does not show any distinct peak in 1981 compared to other years. The peaks in 1995 and 2005 are different. Here, high current speed seems to be the most contributing factor, as the average flow speed shows a distinct peak in winter 1995 and a smaller peak in winter 2005, while the average temperatures show no distinct peaks in those two winters. This suggests a strong connection with inflow from the Arctic or a larger flow in the Greenland Sea Gyre, rather than a connection with a high Atlantic inflow in the Svinøy section. Thus, the driving force of this anomalously high volume transport may be found within the Nordic Seas or in the Arctic.

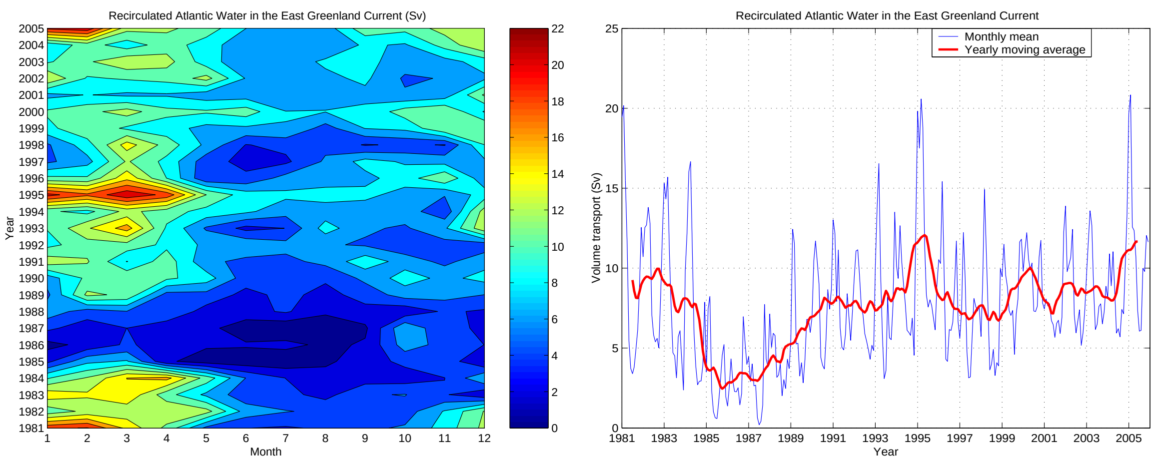

Figure 9.2: ***Volume transports of water with temperatures above 0 ^{o}C, below 30 meters, in the East Greenland Current.***

On average, the model gives a volume transport of 7.7 Sv of water warmer than 0 ^{o}C in the East Greenland Current, using monthly means. The standard deviation is as high as 4.0 Sv, indicating a high variability in the flow. Figure 9.2 shows that this variability is mostly due to seasonal variations, but the interannual variations may also be considerable. Especially in the mid-1980s, it seems to be an anomalously low transport of these water masses, which compares well with the generally reduced transport in the Nordic Seas in that period. The calculated transport compares well with the findings of Woodgate et al. (1999). From a 9-month period of measurements, they calculated an average transport of 8 Sv, with a variance of 4 Sv and an uncertainty of 1 Sv. They found no clear seasonal signal, with the annual variability being on the same order as the shorter time-scale variations. Calculating the transport of recirculated Atlantic Water in the period July 1994-June 1995, gives an average transport of 11.2 Sv, which is about 30% larger than the observed values found by Woodgate et al. (1999). However, considering the 4 Sv variance in the observations by Woodgate et al. (1999) and a standard deviation as high as 6 Sv in the model data, does not give any statistical evidence for a significantly difference in the observed and modeled volume transports.

Looking at the amount of water of Atlantic origin in the Jan Mayen Current, flowing eastward north of Jan Mayen, shows that about two thirds of the Atlantic Water in the East Greenland Current is recirculated into the Greenland Sea basin. On average, 5.6 Sv of water with Atlantic origin is recirculating into the Greenland Sea north of Jan Mayen. The large variations in the Jan Mayen Current, which is directly fed by the East Greenland Current, is also apparent in the standard deviation of the volume transport in the Atlantic layer, with the standard deviation being almost 60% of the total flow. The interannual signal with a very high flow in early 1981, a very low flow in the mid-1980s, and then increasing towards the 1990s, and then oscillating with periods of a few years in later years, is also seen in the Atlantic layer in the Jan Mayen Current (not shown). As two thirds of the water in the Atlantic layer in the East Greenland Current is recirculated into the Greenland Sea Gyre, the remaining one third is expected to enter the Iceland Sea basin between Iceland and Jan Mayen and either enter the Norwegian Sea or leave the Nordic Seas through the Denmark Strait. The outflow of water of Atlantic origin in the Denmark Strait and in the section between Iceland and Jan Mayen is not quantified. However, 1.6 Sv is entering the Nordic Seas through the Denmark Strait, while there is a net westward flow of 2 Sv between Iceland and Jan Mayen. This leaves 0.4 Sv to originate from the East Greenland Current. It is uncertain how large fraction of this is of Atlantic origin.

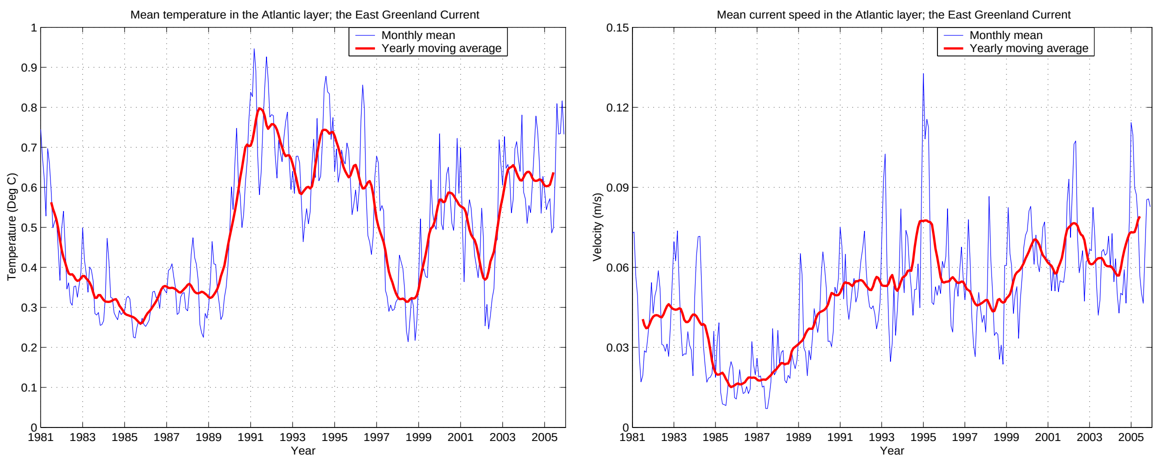

Figure 9.3: ***Mean temperature (left) and mean current speed (right) in the Atlantic layer in the East Greenland Current.***

In the East Greenland Current, the generally lower volume transport in the 1980s is due to both lower temperatures and flow speeds (figure 9.3). The average temperature in the Atlantic layer shows a remarkable variability. In the mid-1980s, the yearly mean temperature is 0.25 to 0.4 ^{o}C. The monthly averaged temperatures never exceeds 0.5 ^{o}C between 1983 and 1989. In 1990, the temperature curve rises sharply, and the yearly mean temperature is 0.6 to 0.8 ^{o}C between 1990 and 1996. Even the monthly averaged temperatures rarely drop below 0.5 ^{o}C in this period. Between 1997 and the end of the data set in 2005, other similar highs and lows are seen. However, these highs and lows last for a shorter period, around 1-3 years. Figure 9.3 may explain the 0.5 ^{o}C increase in temperature in the Denmark Strait overflow between 1999 and 2003, observed by Macrander et al. (2005). The low volume transport of recirculated Atlantic Water in the mid-1980s, may be in connection with the low and highly variable Atlantic inflow in the western branch of the Svinøy section in the 1980s. As this branch of the Atlantic inflow follows the polar front along the eastern slope of the Mohn Ridge and then further along the western slope of the Knipowich Ridge (Orvik & Niiler 2002), this branch may contribute the most to the recirculation of Atlantic Water in the Fram Strait. However, most likely it is also connected with the generally lower volume fluxes in the Nordic Seas in the 1980s.

Chapter 10

Heat fluxes

The heat released from the ocean and into the atmosphere in the Nordic Seas is having a major impact on the climate in northern Europe. In this chapter, the modeled amount of heat transported into the Nordic Seas over the Greenland-Scotland Ridge, will be quantified. Further, the heat flux into the Arctic and the heat loss in the Nordic Seas is calculated. A reference level of zero degrees has been chosen, which means that the Atlantic Water is supposed to have a temperature of 0 ^{o}C when leaving the Nordic Seas. The heat flux is calculated by the equation:

$$Q = Cp * \rho * T * V, \tag{10.1}$$

where Cp is the specific heat capacity of sea water (3985 J/kgK), ρ is the density of sea water (here set to 1028), T is the average temperature (in degrees Celsius, referred to the reference level of zero degrees) and V is the volume flux through the section.

10.1 results

Figures 10.1 and 10.2 show the heat fluxes through the different sections studied in this work. All figures, except for the Fram Strait, are based on the contribution from Atlantic Water only. On the Greenland-Scotland Ridge and in the Svinøy section, Atlantic Water is defined by temperatures above 5 ^{o}C. In the Barents Sea, the temperature for Atlantic Water is set to 3 ^{o}C, and in the East Greenland Current Atlantic Water, or water of Atlantic origin, is defined as water with temperatures above 0 ^{o}C.

Figure 10.1 shows that the heat flux has the same pattern as the volume flux. There is a large seasonal variability in all sections, and there is also a large year to year variation. In the Denmark Strait, the net northward heatflux due to Atlantic inflow is zero at a few occasions. This occurs when there is no water masses classified as Atlantic Water entering through this this section. In the 25-year period modeled, the average heat flux over the Greenland-Scotland Ridge is 159 TW through the Faroe-Shetland Channel, 96 TW over the Iceland-Faroe Ridge and 22 TW through the Denmark Strait, a total of 277 TW. There is, however, large year to year variations, with values ranging from a minimum of 158 TW in May 1987 to 448 TW in January 1989. Using yearly averages from July to June, show that the lowest heat flux is is taking place in 1985/86, with a yearly average of 236 TW. The

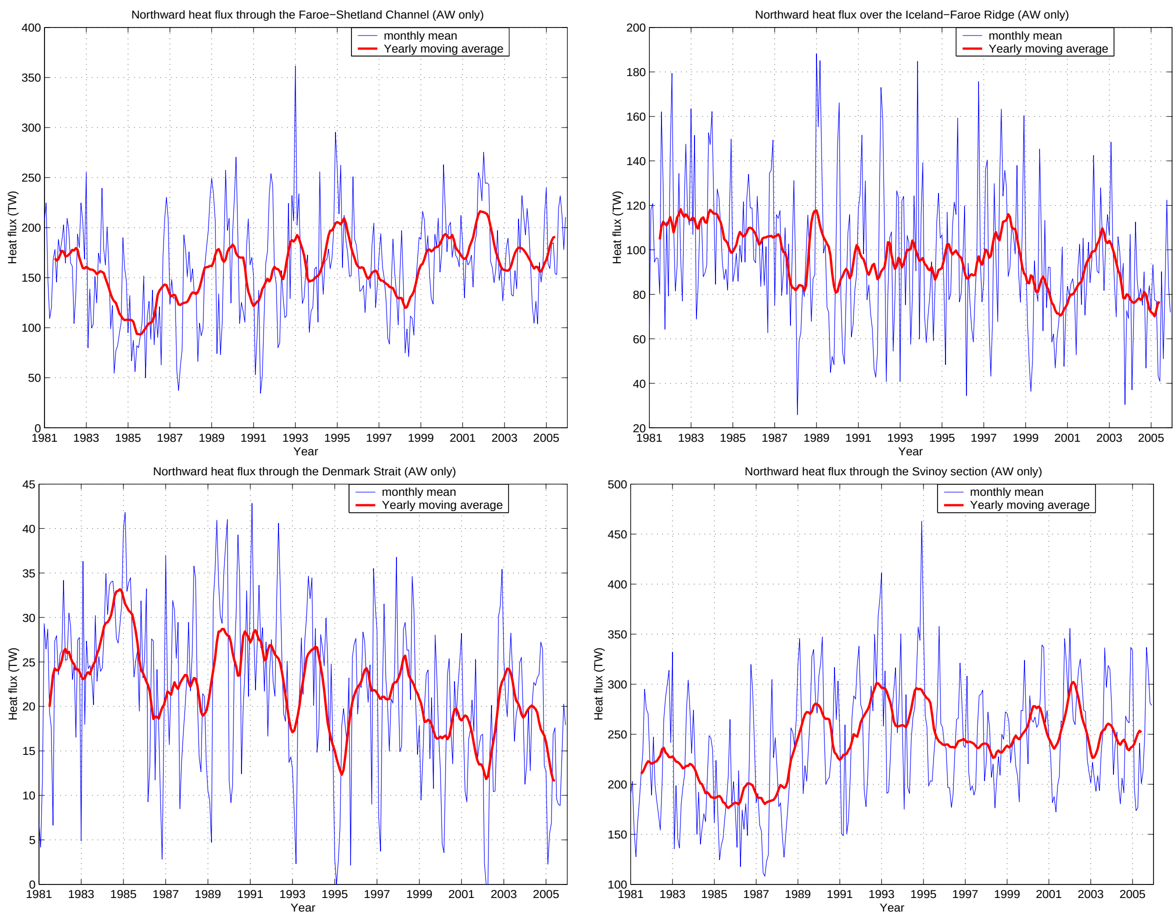

Figure 10.1: ***Heat fluxes into the Nordic Seas through the Faroe-Shetland Channel (top left), Iceland-Faroe section (top right), Denmark Strait (bottom left) and Svinøy section (bottom right). All values are relative to 0 ^{o}C and only contribution from Atlantic Water is included. Note the scaling.***

largest heat flux ocurrs in 2001/02 with a yearly average of 325 TW. Downstream of the Atlantic inflow over the G-S Ridge, in the Svinøy section, the average heat flux is 239 TW. The heat flux through the Svinøy section reflects the volume transport through the section, with a distinct shift between the 1980s and 1990s (figure 10.1). Including only the years 1981-1989, gives an average heat flux of 210 TW, while including only the years after 1989, gives an average heat flux of 256 TW. In December 1994, there is a distinct peak and the heat flux reaches 463 TW, which is the highest value found in the whole time series. This is related to the very high volume transport through the section in December 1994.

Figure 10.2 reveals a tremendous variability in the northward heat flux through the Fram Strait, with yearly averages ranging from 9 TW in (1985/86) to 74 TW in 1989/90 and 1994/95. On a monthly time scale, the values range from 4 TW (June 1997) to 139 TW (January 1995). For the whole time series, the average heat flux is 42 TW northward and -4 TW southward. This gives an average net heat flux of 46 TW into the Arctic through the Fram Strait. Also the East Greenland Current exhibits very large variations in heat content, both on monthly and yearly time scales (figure 10.2). There is a typical seasonal pattern, but the amplitudes are varying greatly from year to year, with a period of very low heat fluxes in the mid-1980s and a period of very large heat fluxes in the early and mid-1990s. The heat flux into the Barents Sea differs substantially from the heat flux through the Fram Strait. There is a clear seasonal signal with large differences interannually. However, the yearly mean is very stable (figure 10.2). Averaged over the modeled period, the net heat flux from Atlantic Water into the Barents Sea is 98 TW, with a standard deviation of 34 TW. However, based on yearly averages, the average heat flux is 98 TW with a standard deviation of only 8 TW.

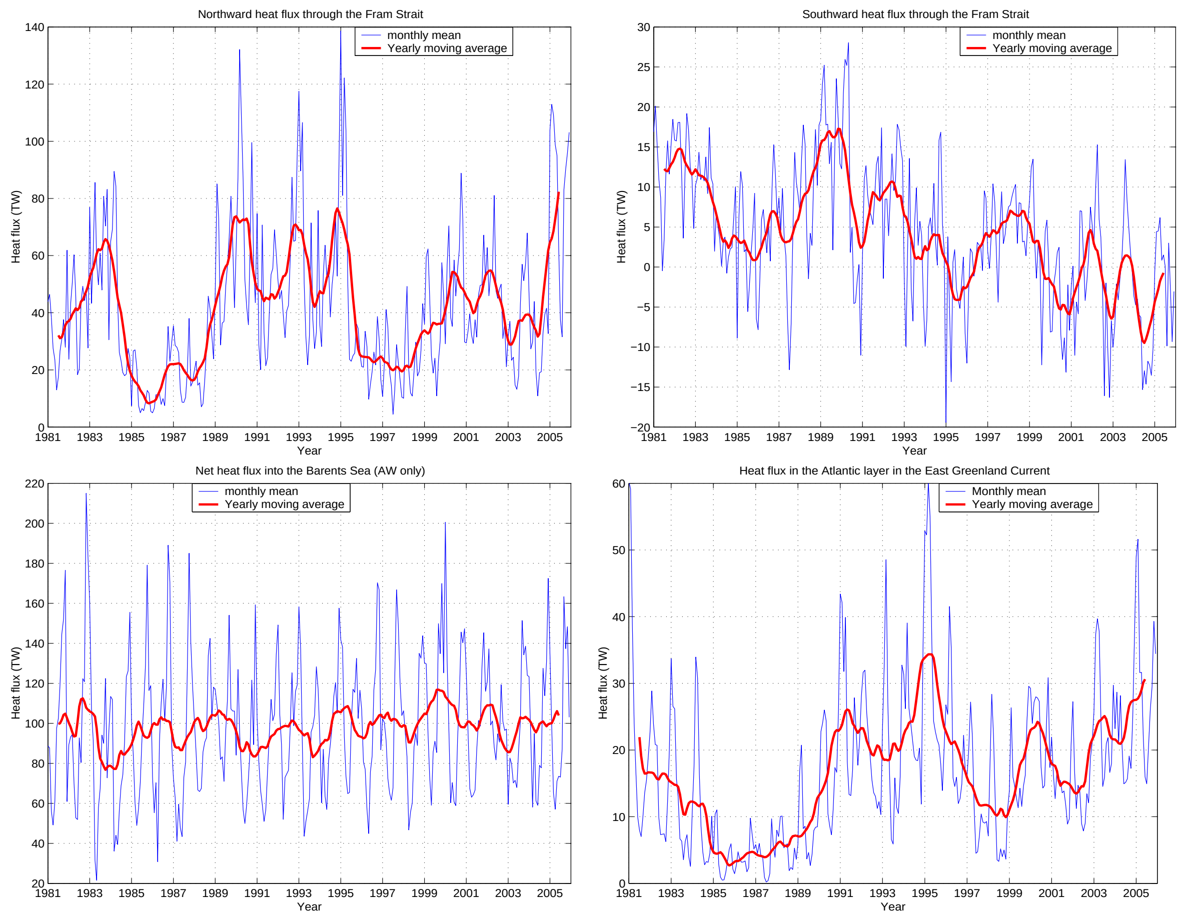

Figure 10.2: ***Northward (upper left) and southward (upper right) heat flux through the Fram Strait (positive values northward). Eastward heat flux into the Barents Sea (lower left) and southward heat flux in the East Greenland Current (lower right). All values are relative to 0 °C. In lower panel only contribution from Atlantic Water is included. Atlantic Water is defined as temperature above 0 °C in the East Greenland Current, and 3 °C in the Barents Sea. Note the different scaling in the plots.***

10.2 Discussion

Volume fluxes, average temperatures and heat fluxes in the different sections are shown in table 10.1. The largest contributor to the heat flux into the Nordic Seas is the inflow through the Faroe-Shetland Channel. This is mostly due to higher average temperature in this section. The contribution from the inflow over the Iceland-Faroe Ridge is less, although the volume transport is almost equal in the two sections (table 5.1). The inflow through the Denmark Strait is by far the smallest contributor, with only one tenth of the total heat flux over the G-S Ridge. According to the model results, there is a net heat loss of 38 TW between the Greenland-Scotland Ridge and the Svinøy section. Calculating the volume transport and heat flux over the Greenland-Scotland Ridge in the years 1999-2001, which are the years Østerhus et al. (2005) based their calculations on, gives a modeled net volume transport of Atlantic Water into the Nordic Seas of 7.6 Sv and a heat flux of 282 TW. Computing the heat flux through the Svinøy section in the same period gives 255 TW, which indicates a 10 percent net heat loss between the Greenland-Scotland Ridge and the Svinøy section. However, possible recirculation in the Svinøy section is not subtracted from the total Atlantic inflow in this section, which may contribute to a higher calculated heatflux through the Svinøy section.

Orvik & Skagseth (2005) estimated a heat flux in the eastern branch of the Noerwgian Atlantic Current of 133 TW (table 10.1). To extend the observed heat flux through the Svinøy section to include the western branch of the Norwegian Atlantic Current, the same temperature as the observed temperature in the eastern branch (7.8 ^{o}C) is used. Then, using the observed volume transport of 3.4 Sv (Orvik et al. 2001), gives a heat flux of 109 TW in the western branch. This gives a total heat flux of 242 TW through the Svinøy section. However, the uncertainty in this number must include that the western branch mainly consists of Atlantic Water from the inflow between Greenland and the Faroes (Orvik & Niiler 2002), which has a slightly lower temperature than the inflow through the Faroe-Shetland Channel (Østerhus et al. 2005). In addition, this "one-box method" gives only a crude estimate of the heat transport. Therefore, the calculated heat flux in the western branch presented here may be too high. The western branch is also a more variable current, which contributes to a large uncertainty in the volume flux and therefore also in the heat flux. Compared to the heat fluxes observed over the Greenland-Scotland Ridge (Østerhus et al. 2005), the results suggest that there is a heat loss of 20 percent between the Greenland-Scotland Ridge and the Svinøy section.

The total heat flux through the Fram Strait, and also southward in the East Greenland Current, show a large variability both seasonally and interannually, in contrast to the heat flux into the Barents Sea, which shows a large seasonal variability, but a rather constant value at longer time scales. In the Fram Strait and the East Greenland Current, the mid-1980s are seen as a period of low heat flux, while the mid-1990s are seen as a period of high heat flux. This is in agreement with the findings of Quadfasel et al. (1991) and Grotefendt et al. (1998), reporting a warming of 1 ^{o}C in the intermediate/Atlantic layer in the Arctic. In figure 10.2, it is seen that there was a dramatic increase in the heat transport into the Arctic between 1988 and 1991. In 1995, after the highest peak in the whole time series, the heat flux almost dropped back to the values before 1989, until the increase observed by Schauer et al. (2004)

is seen, starting in 1998. Schauer et al. (2004) observed an increase in the annual mean net heat flux from 16 TW in 1997/98 to 41 TW in 1998/99. The corresponding values in the model are 25 TW and 39 TW, respectively.

Simonsen & Haugan (1996) concluded that the net heat flux into the Arctic is most likely in the range 50-80 TW. However, this estimate includes southward ice-transport, which is not included in the numbers discussed above. According to Simonsen & Haugan (1996), the heat transport of latent heat due to ice-export, is in the range 21-54 TW. The major part of the heat transport occurs in the Fram Strait. Therefore, the modeled net northward heat flux of 46 TW, obtained from the whole modeled time series, should lie within this range.

	Modeled			Observations			
Section	Vol	Heat	Av T	Vol	Heat	Av T	Period
F-S Channel	4.2	185	9.5	3.8[1]	156[1]	9.5[1]	1999-2001
Iceland-Faroe Ridge	2.7	79	7.3	3.8[1]	134[1]	8.2[1]	1999-2001
Denmark Strait	0.7	18	6.2	0.8[1]	22[1]	6.0[1]	1999-2001
Total G-S Ridge	7.6	282	8.4	8.5[1]	313[1]	8.5[1]	1999-2001
Svinøy section, tot	7.0	239	8.7				1981-2005
Svinøy section, EB	3.8	147	9.5	4.2[2]	133[2]	7.8[2]	1996-2005
Svinøy section, WB	3.6	103	7.4				1996-2005
Fugl.-Bjørn.	4.6^{+}	98	5.9				1981-2005
Fram Strait	9.2^{+}	12	1.7	9.5^{+}[3]	25[3]		1997-1999
Greenland East	7.5	18	0.5				1981-2005
Jan Mayen N	5.5	12	0.5				1981-2005

Table 10.1: ***Volume fluxes, heat fluxes and average temperature in the Atlantic layer in different sections in the Nordic Seas. Volume fluxes are given in Sverdrup (1 Sv = 10^6 $m^3 s^{-1}$), heat fluxes are given in Tera Watt (TW = 10^{12} W) relative to $0^o C$, only contribution from Atlantic Water is included. $^{+}$Total northward/eastward transport. [1]Østerhus et al, 2005; [2]Orvik and Skagseth, 2005; [3]Schauer et al, 2004.***

The volume fluxes of Atlantic Water over the G-S Ridge, and thus also the heat fluxes, are low compared to observations (table 10.1). The observations are from Østerhus et al. (2005). Based on existing literature, Simonsen & Haugan (1996) concluded that the heat flux into the Nordic Seas is probably around 300 TW. With a heat flux in the range 50-80 TW into the Arctic Ocean, the net heat flux into the Nordic Seas is in the range 220-250 TW. Here the Barents Sea is included in the Nordic Seas. An estimate of the heat loss in the Barents Sea yields a heat loss in the range 28-80 TW (Simonsen & Haugan 1996). This gives a net heat loss in the Nordic Seas (excluding the Barents Sea) of 140-222 TW, when the heat flux between the Barents Sea and the Arctic is neglected. The corresponding heat budget obtained in the model gives a heat transport from the Atlantic into the Nordic Seas of 277 TW. The net heat flux into the Barents Sea is 98 TW and 27 TW is transported northward through the Fram Strait, which gives a net heat loss of 152 TW in the Nordic Seas. This low number may be explained by the lower than observed inflow over the Greenland-Scotland

Ridge and the higher than observed outflow to the Barents Sea. The low values compared to recent observations, may also be partly explained by the generally lower modeled circulation in the Nordic Seas in the 1980s, which are included in this budget.

Table 10.1 shows that the modeled southward heat flux in the Atlantic layer in the East Greenland Current is 18 TW, averaged over the whole period 1981-2005. Similar calculations for the Jan Mayen Current shows an eastward heat flux of 12 TW north of Jan Mayen, which agrees with the finding that 2/3 of the recirculated or modified Atlantic Water in the East Greenland Current recirculates into the Greenland Sea.

Chapter 11

Salinity

Salinity is an important part of the water mass characteristic and is influencing the density of seawater. Therefore, salinity is often used to define water masses. However, the salinity is not always well resolved in models, especially near the surface, where the influence from the atmosphere is large. Here, some results of the modeled salinity are shown, and the behavior of the salinity in this model run is discussed in short terms. Figure 11.1 shows the yearly averaged sea surface salinity in the Nordic Seas. There is no clear trend in the sea surface salinity, although the mid-1980s are seen as a period of lower salinity than the rest of the modeled period. This low might be in connection with the lower Atlantic inflow in that period. Despite the fact that the earlier mentioned sign error in the evaporation will actually treat evaporation as precipitation, the sea surface salinity shows a rather stable mean, except for the already mentioned period in the 1980s. Thus, there seems to be a drift towards higher salinity in the model that is masked by the precipitation/evaporation error. However, looking at hydrographic sections through the Atlantic inflow, reveals that salinity is decreasing with time, at such a rate that after a period of 15 years, water masses with salinity above 35.0 psu is absent from the core of the Atlantic inflow. This freshening of the surface is mixed deeper into the ocean as time evolves, and is thereby contaminating the upper part of the water column, figure 11.2. In 1985, after the model has run for 5 years, a layer of water with salinity below 34 psu is seen down to about 50 meter depth in the Norwegian Sea. Near the shelf, a core of water with salinity above 35.0 psu (equivalent with Atlantic Water) is still seen in 1985. By 1995, the core of Atlantic Water has disappeared, and by 2005, the layer of relatively fresh water in the Norwegian Sea has reached down to about 500 meter depth. Only the deep water masses (below 1000 m) are still unaffected by the unrealistic changes in salinity.

The results in figures 11.1 and 11.2 may seem contradictory. However, figure 11.3 shows that there are regional differences in the changes of the sea surface salinity. It is clearly seen that the shelf areas, such as the North Sea and the norwegian coast are getting more saline as time evolves. The reason why the North and Baltic Seas are left blank, is that the values in these areas are outside the range. However, the anomaly in 2004 is just within the range of 3 psu. When calculating the average sea surface salinity shown in figure 11.1, the Baltic Sea and eastern part of the North Sea is left out, because of the large anomalies in these

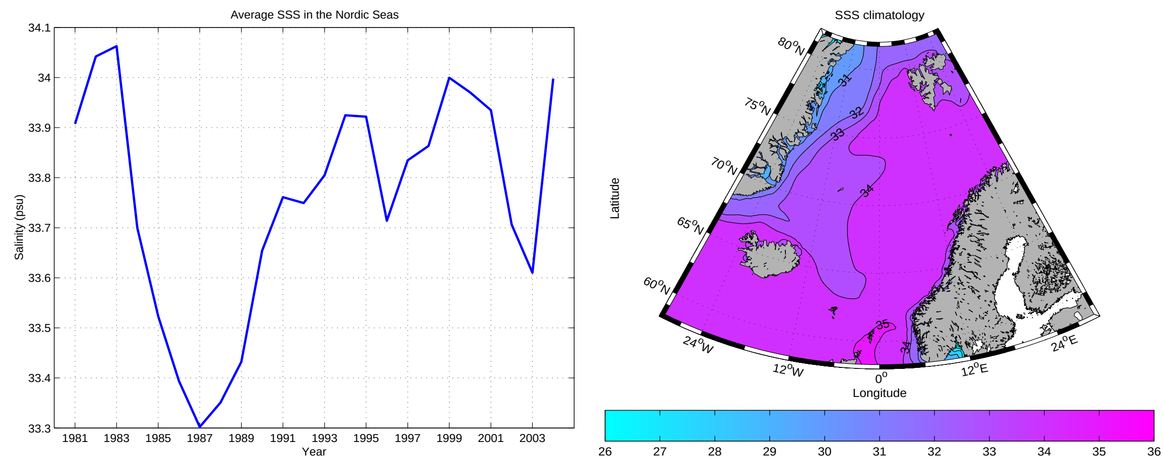

Figure 11.1: ***Left: Yearly average sea surface salinity in the Nordic Seas. Right: Climatological sea surface salinity, based on model results from 1981 to 2004.***

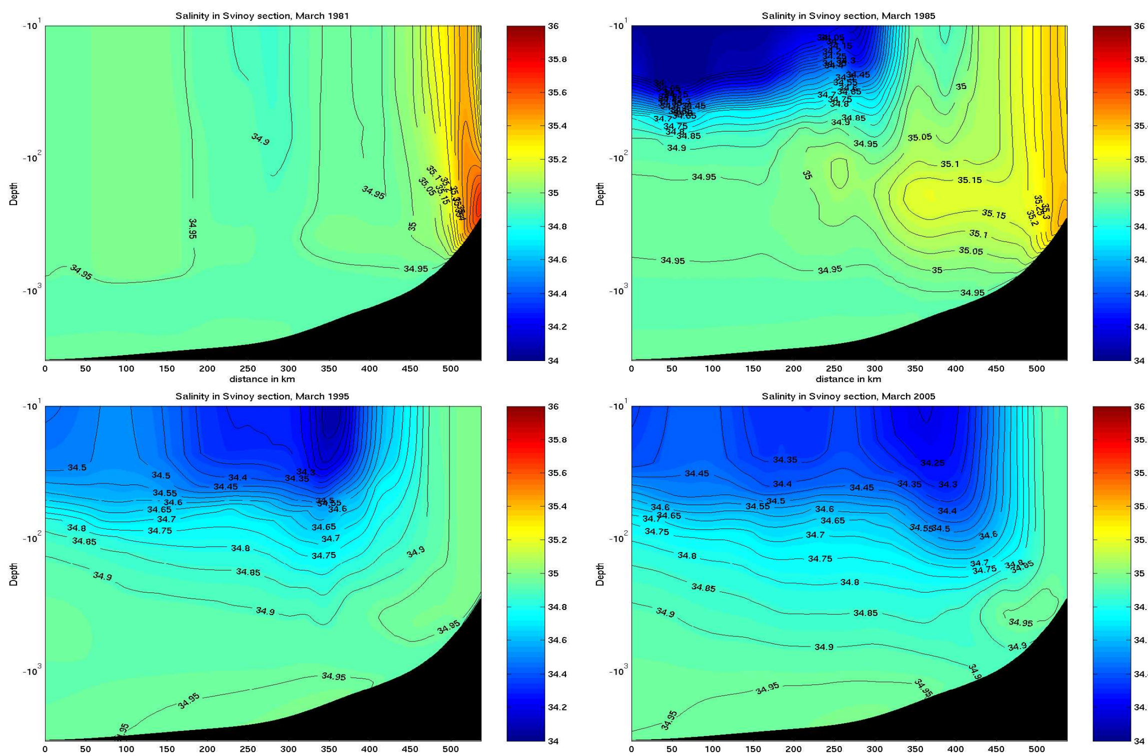

Figure 11.2: ***Salinity in Svinøy section in 1981 (upper left), 1985 (upper right), 1995 (lower left) and 2005 (lower right).***

areas, and because these areas are outside the area of interest in this study. From figure 11.3, it is clear that the sea surface in the Greenland Sea, and especially the western part, is getting more saline, while the Norwegian Atlantic Current is freshening. Thus, the sea surface salinity is more homogenous throughout the Nordic Seas at the end of the model run. This is not a surprising result. The sign error in the evaporation will have the largest impact in tropical regions, due to the higher temperatures and therefore higher evaporation rates at lower latitudes. Thus, too fresh water masses are pumped into the Nordic Seas through the Atlantic inflow over the Greenland-Scotland Ridge, as seen in figures 11.2 and 11.3.

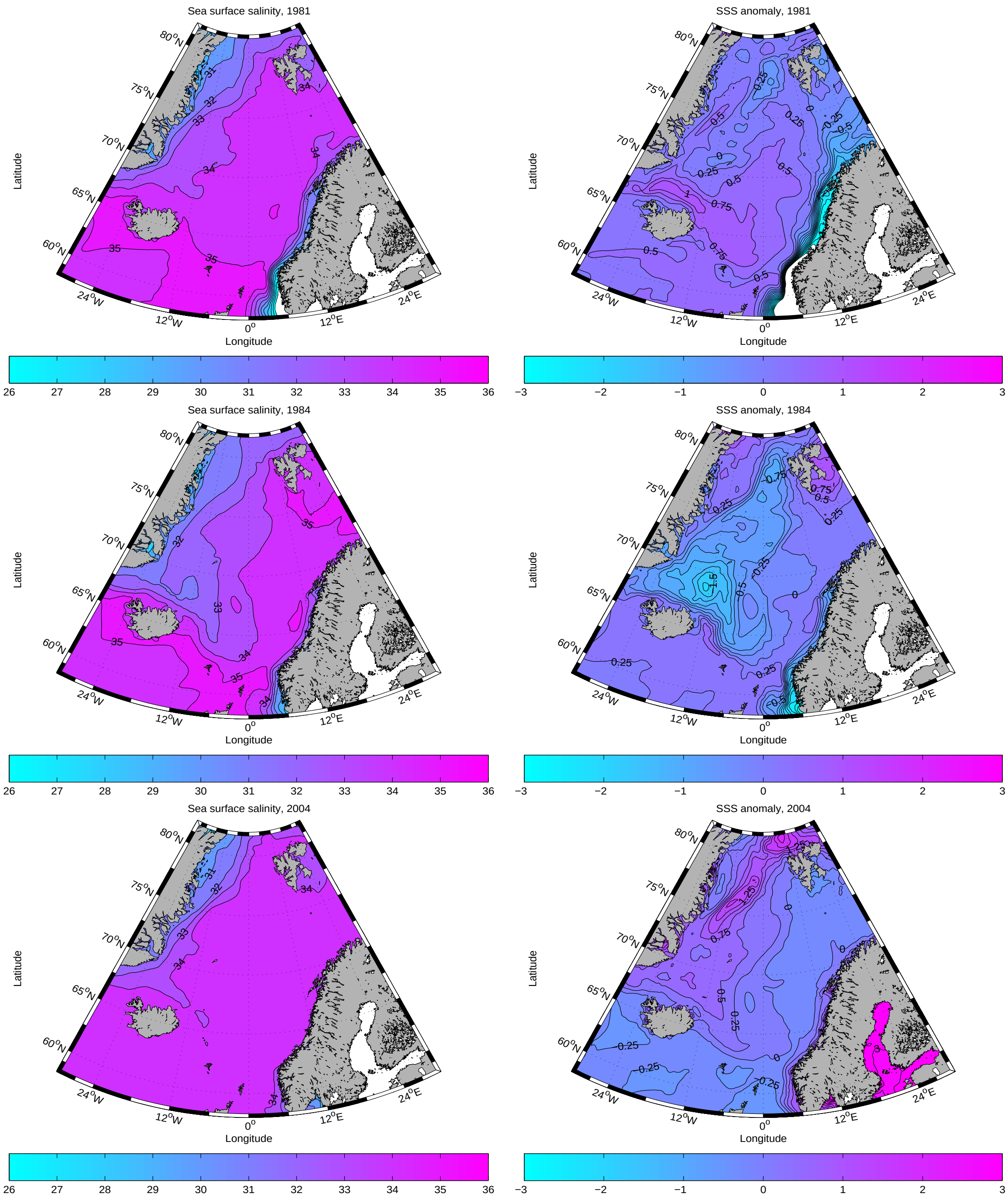

Figure 11.3: ***Sea surface salinity (left) and sea surface salinity anomaly (right) in 1981 (upper panel), 1984 (middle panel) and 2004 (lower panel).***

Chapter 12

Concluding remarks

The model gives a good representation of the general circulation pattern within the Nordic Seas basin and the exchanges between the Atlantic and the Arctic. In all key sections investigated, except the Barents Sea Opening, the modeled volume transports are within the error limits of the observations. However, the variability on both monthly and yearly time scales is larger in the model than in the observations. The two pathways for the Atlantic Water into the Arctic are substantially different. The northward flow of Atlantic Water through the Fram Strait is highly variable with large year to year variations, while the eastward flow of Atlantic Water into the Barents Sea shows only large seasonal variability and is nearly constant on longer time scales. Some of the variability in the Fram Strait is in agreement with recent observations of an increased inflow of Atlantic Water and a warming in the Arctic.

A shift of regime is seen in the model between the 1980s and 1990s, when the general circulation is intensified. During this intensification, the western branch of the Norwegian Atlantic Current is established as a distinct current which persists throughout the rest of the modeled period. This also influences the recirculation of Atlantic Water in the Fram Strait and downstream in the East Greenland Current.

Budgets of volume and heat transports through the Nordic Seas are presented and compared to observations. The modeled heat sink in the Nordic Seas (excluding the Barents Sea) is in the lower end of estimates based on observations. Two main factors contribute to this; the Atlantic inflow over the Greenland-Scotland Ridge is slightly lower in the model than in observations, and the modeled volume transport of Atlantic Water into the Barents Sea is significantly higher than in observations. While the temperatures are very close to observed values, the lower Atlantic inflow into the Nordic Seas is due to lower than observed northward volume transports over the Greenland-Scotland Ridge.

Overall, the model does an excellent job in reproducing the general circulation pattern in the Nordic Seas, and the accuracy in bulk fluxes is sufficient for producing realistic volume and heat budgets for the Nordic Seas. However, the model resolution is too coarse when looking at smaller than basin-scale processes, and the low accuracy in the salinity makes it impossible to separate water masses by salinity.

Bibliography

Bentsen, M. & Drange, H. (2000), 'Parameterizing surface fluxes in ocean models using the NCEP/NCAR reanalysis data. In: Regclim General Technical Report No 4, Norwegian Institute for Air Research, Kjeller, Norway', pp. 44–57.

Bentsen, M., Evensen, G., Drange, H. & Jenkins, A. D. (1999), 'Coordinate transformation on a sphere using conformal mapping', *Mon. Weather Rev* **127**, 2733–2740.

Budgell, W. P. (2005), 'Numerical simulation of ice-ocean variability in the Barents Sea region; Towards dynamical downscaling', *Ocean Dynamics* **55**, 370–387.

Dickson, B., Meincke, J., Vassie, I., Jungclaus, J. & Østerhus, S. (1999), 'Possible predictability in overflow from from the Denmark Strait', *Nature* **397**, 243–246.

Dickson, R. R. & Brown, J. (1994), 'The production of North Atlantic Deep Water: Sources, rates and pathways', *J. Geophys. Res.* **99**, 12319–12341.

Dickson, R. R., Osborn, T. J., Hurrell, J., Meincke, J., Blindheim, J., Ådlandsvik, B., Vinje, T., Alekseev, G. & Maslowski, W. (2000), 'The Arctic Ocean response to the North Atlantic Oscillation', *J. Clim.* **15**, 2671–2696.

Fahrbach, E., Heinze, C., Rohardt, G. & Woodgate, R. A. (1995), 'Moored current meter measurements in the East Greenland Current', *in Nordic Seas Symposium on the Results of the Greenland Sea Project (GSP) 1987-1993, Extended Abstracts, edited by J. Meincke. Inst. für Meereskunde, Hamburg, Germany* pp. 57–60.

Fahrbach, E., Meincke, J., Østerhus, S., Rohardt, G., Schauer, U., Tverberg, V. & Verduin, J. (2001), 'Direct measurements of volume transports through Fram Strait', *Polar Res.* **20**, 217–224.

Fissel, D., Birch, J., Melling, H. & Lake, R. (1988), 'Non-tidal flows in the North-west Passage', *Tech. Rep.* **98**, Canadian Institute of Ocean Science, Sidney, British Columbia, Canada.

Foldvik, A., Aagaard, K. & Tørresen, T. (1988), 'On the velocity field of the East Greenland Current', *Deep-Sea Res.* **35**, 1335–1354.

Girton, J. B., Sanford, T. B. & Kase, R. H. (2001), 'Synoptic sections of the Denmark Strait overflow', *Geophys. Res. Lett.* **28**, 1619–1622.

Grotefendt, K., Logemann, K., Quadfasel, D. & Ronski, S. (1998), 'Is the Arctic Ocean warming?', *J. Geophys. Res.* **103**, 27679–27687.

Haidvogel, D. B., Arango, H. G., Hedstrøm, K., Beckmann, A., Malanotte-Rizoli, P. & Shchepetkin, A. F. (2000), 'Model evaluation experiments in the North Atlantic Basin: Simulations in nonlinear terrain-following coordinates', *Dyn. Atmos. Oceans* **32**, 239–281.

Haidvogel, D. B. & Beckmann, A. (1999), 'Numerical Ocean Modelling', *Imperial College Press, London* .

Hansen, B. & Østerhus, S. (2000), 'North Atlantic-Nordic Seas Exchanges', *Prog. Oceanog.* **45**, 109–208.

Hansen, B., Østerhus, S., Hátún, H., Kristiansen, R. & Larsen, K. M. H. (2003), 'The Iceland-Faroe inflow of Atlantic water to the Nordic Seas', *Prog. Oceanog.* **59**, 443–474.

Helland-Hansen, B. & Nansen, F. (1909), 'The Norwegian Sea: Its Physical Oceanography based upon the Norwegian Research 1900-1904, Part 1, No. 2', *Fiskeridir. Skr. Ser. Havunders.* **3**, 390pp.

Hilmer, M. & Jung, T. (2000), 'Evidence for a recent change in the link between the North Atlantic Oscillation and the Arctic sea ice transport', *Geophys. Res. Lett.* **27**, 989–992.

Ingvaldsen, R., Asplin, L. & Loeng, H. (2004), 'The seasonal cycle in the Atlantic transport to the Barents Sea during the years 1997-2001', *Cont. Shelf Res.* **24**, 1015–1032.

Jonsson, S. & Valdimarsson, H. (2004), 'A new path for the Denmark Strait overflow water from the Iceland Sea to Denmark Strait', *Geophys. Res. Lett.* **31 (3)**.

Kalnay, E., Kanamitsu, M., Kistler, R., Collins, W., Deaven, D., Gandin, L., Iredell, M., Saha, S., White, G., Woollen, J., Zhu, Y., Chelliah, M., Ebisuzaki, W., Higgins, W., Janowiak, J., Mo, K. C., Ropelewski, C., Wang, J., Leetma, A., Reynolds, R., Jenne, R. & Joseph, D. (1996), 'The NCEP/NCAR 40-year reanalysis project', *Bull. Amer. Met. Soc.* **77(3)**, 437–471.

Large, W. G., McWilliams, J. C. & Doney, S. C. (1994), 'Oceanic vertical mixing: A review and a model with a nonlocal boundary layer parameterization', *Rev. Geophys.* **32**, 10937–10954.

Legutke, S. (1991), 'A numerical investigation of the circulation in the Greenland and Norwegian Seas', *J. Phys. Oceanogr.* **21**, 118–148.

Macrander, A., Send, U., Valdimarsson, H., Jnsson, S. & Kase, R. H. (2005), 'Interannual changes in the overflow from the Nordic Seas into the Atlantic Ocean through Denmark Strait', *Geophys. Res. Lett.* **32**, L06606.

Maslowski, W., Marble, D., Walczowski, W., Schauer, U., Clement, J. L. & Semtner, A. J. (2004), 'On climatological mass, heat and salt transports through the Barents Sea and Fram Strait from a pan-Arctic couples sea-ice model simulation', *J. Geophys. Res.* **109**, C03032.

Mork, K. A. & Blindheim, J. (2000), 'Variation in the Atlantic Inflow to the Nordic Seas, 1955-1996', *Deep-Sea Res. I* **47**, 1035–1057.

Nilsen, J. E. ø., Gao, Y., Drange, H., Furevik, T. & Bentsen, M. (2003), 'Simulated North Atlantic-Nordic Seas water mass exchanges in an isopycnic coordinate OGCM', *Geophys. Res. Lett.* **30**, 4.

Oki, T. & Sud, Y. C. (1998), 'Design of a Total Runoff Integrating Pathways (TRIP): A global river channel network', *Earth Interactions* **2**.

Orvik, K. A. & Niiler, P. (2002), 'Major pathways of Atlantic water in the northern North Atlantic and Nordic Seas toward Arctic', *Geophys. Res. Lett.* **29**, 4.

Orvik, K. A. & Skagseth, Ø. (2005), 'Heat flux variations in the eastern Norwegian Atlantic Current toward the Arctic from moored instruments, 1995-2005', *Geophys. Res. Lett.* **32**.

Orvik, K. A., Skagseth, ø. & Mork, M. (2001), 'Atlantic inflow to the Nordic Seas: current structure and volume fluxes from moored current meters, VM-ADCP and SeaSoar-CTD observations, 1995-1999', *Deep-Sea Res.* **48**, 937–957.

Østerhus, S., Turrell, W. R., Jnsson, S. & Hansen, B. (2005), 'Measured volume, heat and salt fluxes from the Atlantic to the Arctic Mediterranean', *Geophys. Res. Letters* **32**, 4 pp.

Quadfasel, D., Sy, A., Wells, D. & Tunik, A. (1991), 'Warming in the Arctic', *Nature* **350**.

Schauer, U., Fahrbach, E., Østerhus, S. & Rohardt, G. (2004), 'Arctic warming through the Fram Strait: Oceanic heat transport from 3 years of measurements', *J. Geophys. Res.* **109**, 14.

Shchepetkin, A. F. & McWilliams, J. C. (2003), 'A method for computing horizontal pressure-gradient force in an oceanic model with a nonaligned vertical coordinate', *J. Geophys. Res.* **108**.

Shchepetkin, A. F. & McWilliams, J. C. (2005), 'The Regional Ocean Modeling System (ROMS): A split-explicit, free-surface, topography-following coordinates ocean model', *Ocean Modelling* **9**, 347–404.

Simonsen, K. & Haugan, P. M. (1996), 'Heat budgets of the Arctic Mediterranean and sea surface heat flux parametrizations for the Nordic Seas', *J. Geophys. Res.* **101**, 6553–6576.

Song, Y. & Haidvogel, D. B. (1994), 'A semi-implicit ocean circulation model using a generalized topography-following coordinate system', *J. Comput. Phys.* **115**, 228–244.

Stevens, D. P. (1991), 'A numerical ocean circulation model of the Norwegian and Greenland Seas', *Prog. Oceanogr.* **27 (3-4)**, 365–402.

Turrell, W. B., Hansen, B., Hughes, S. & østerhus, S. (2003), 'Hydrographic variability during the decade of the 1990's in the northeastern Atlantic and southern Norwegian Sea', *ICES Mar. Sci. Symp.* .

Woodgate, R. A., Fahrbach, E. & Rohardt, G. (1999), 'Structure and transports of the East Greenland Current at 75 degrees N from moored current meters', *J. Geophys. Res.-Oceans* **104**, 18059–18072.

Worthington, L. V. (1970), 'The Norwegian Sea as a Mediterranean basin', *Deep Sea Res.* **17**, 77–84.

Chapter 13

Appendix

13.1 Abbreviations

Table with abbreviations and coordinates for the different sections shown in the map, figure 3.1.

Section	Abb.	Longitude	Latitude
Denmark Strait	DS	31^oW - 24^oW	68^o30'N - 65^o30'N
Iceland-Faroe Ridge	IF	14^oW - 7^oW	65^oN - 62^oN
Faroe - Orkney/Faroe-Shetland Channel	FO	7^oW - 3^oW	62^oN - 59^oN
Utsira West/Utsira - Orkney	UW	2^o30'W - 5^o30'E	59^o20'N
Svinøy Section	SS	2^oW - 5^oE	66^o30'N - 62^oN
Gimsøy section	GS	2^oW - 14^oE	74^o30'N - 68^oN
Fugløya - Bjørnøya	FB	20^oE - 19^o30'E	70^oN - 74^o30'N
Bjørnøya - Spitsbergen	BS	17^oE - 19^o30'E	76^o30'N - 74^o30'N
Bjørnøya West	BW	2^oW - 19^o30'E	74^o30'N
Fram Strait	FS	20^oW - 11^oE	79^o40'N
Greenland East	GE	20^oW - 8^oW	75^oN - 74^oN
Jan Mayen North	JN	8^oW	71^oN - 74^oN
Iceland - Jan Mayen	IJ	15^oW - 8^oW	66^oN - 71^oN

Table 13.1: ***Abbreviations and coordinates of the different sections.***